SEISMIC HAZARD ZONE REPORT 098

**PRELIMINARY REPORT**
FOR REVIEW PURPOSES ONLY
TO BE SUPERSEDED ON OR ABOUT
October 19, 2004

# SEISMIC HAZARD ZONE REPORT FOR THE NILES 7.5-MINUTE QUADRANGLE, ALAMEDA COUNTY, CALIFORNIA

**2004**

**DEPARTMENT OF CONSERVATION**
***California Geological Survey***

**STATE OF CALIFORNIA**
ARNOLD SCHWARZENEGGER
*GOVERNOR*

**THE RESOURCES AGENCY**
MICHAEL CHRISMAN
*SECRETARY FOR RESOURCES*

**DEPARTMENT OF CONSERVATION**
DARRYL YOUNG
*DIRECTOR*

CALIFORNIA GEOLOGICAL SURVEY
MICHAEL S. REICHLE, *ACTING STATE GEOLOGIST*

Copyright © 2004 by the California Department of Conservation. All rights reserved. No part of this publication may be reproduced without written consent of the Department of Conservation.

"The Department of Conservation makes no warrantees as to the suitability of this product for any particular purpose."

SEISMIC HAZARD ZONE REPORT 098

# SEISMIC HAZARD ZONE REPORT FOR THE NILES 7.5-MINUTE QUADRANGLE, ALAMEDA COUNTY, CALIFORNIA


**CALIFORNIA GEOLOGICAL SURVEY'S PUBLICATION SALES OFFICES:**

Southern California Regional Office
655 S. Hope Street, Suite 700
Los Angeles, CA 90017
(213) 239-0878

Publications and Information Office
801 K Street, MS 14-34
Sacramento, CA 95814-3531
(916) 445-5716

Bay Area Regional Office
185 Berry Street, Suite 210
San Francisco, CA 94107-1728
(415) 904-7707

# CONTENTS

EXECUTIVE SUMMARY ..... vii

INTRODUCTION ..... 1

SECTION 1 LIQUEFACTION EVALUATION REPORT Liquefaction Zones in the Niles 7.5-Minute Quadrangle, Alameda County, California ..... 3

PURPOSE ..... 3

BACKGROUND ..... 4

METHODS SUMMARY ..... 4

SCOPE AND LIMITATIONS ..... 5

PART I ..... 5

PHYSIOGRAPHY ..... 5

GEOLOGY ..... 7

ENGINEERING GEOLOGY ..... 11

GROUND WATER ..... 14

PART II ..... 15

LIQUEFACTION POTENTIAL ..... 15

LIQUEFACTION SUSCEPTIBILITY ..... 16

LIQUEFACTION OPPORTUNITY ..... 17

LIQUEFACTION ZONES ..... 18

ACKNOWLEDGMENTS ..... 21

REFERENCES ..... 22

SECTION 2 EARTHQUAKE-INDUCED LANDSLIDE EVALUATION REPORT Earthquake-Induced Landslide Zones in the Niles 7.5-Minute Quadrangle, Alameda County, California ..... 29

PURPOSE ..... 29
BACKGROUND ..... 30
METHODS SUMMARY ..... 30
SCOPE AND LIMITATIONS ..... 31
PART I ..... 32
PHYSIOGRAPHY ..... 32
GEOLOGY ..... 33
ENGINEERING GEOLOGY ..... 38
PART II ..... 41
EARTHQUAKE-INDUCED LANDSLIDE HAZARD POTENTIAL ..... 41
EARTHQUAKE-INDUCED LANDSLIDE HAZARD ZONE ..... 45
ACKNOWLEDGMENTS ..... 46
REFERENCES ..... 46
AIR PHOTOS ..... 49
APPENDIX A Source of Rock Strength Data ..... 50
SECTION 3 GROUND SHAKING EVALUATION REPORT Potential Ground Shaking in the Niles 7.5-Minute Quadrangle, Alameda County, California ..... 51
PURPOSE ..... 51
EARTHQUAKE HAZARD MODEL ..... 52
APPLICATIONS FOR LIQUEFACTION AND LANDSLIDE HAZARD ASSESSMENTS 56
USE AND LIMITATIONS ..... 59
REFERENCES ..... 60

# ILLUSTRATIONS

Figure 2.1. Yield Acceleration vs. Newmark Displacement for the Lucerne Record for the 1992 Landers Earthquake. .....43

Figure 3.1. Niles 7.5-Minute Quadrangle and portions of adjacent quadrangles, 10 percent exceedance in 50 years peak ground acceleration (g)—Firm rock conditions. .....53

Figure 3.2. Niles 7.5-Minute Quadrangle and portions of adjacent quadrangles, 10 percent exceedance in 50 years peak ground acceleration (g)—Soft rock conditions. .....54

Figure 3.3. Niles 7.5-Minute Quadrangle and portions of adjacent quadrangles, 10 percent exceedance in 50 years peak ground acceleration (g)—Alluvium conditions.....55

Figure 3.4. Niles 7.5-Minute Quadrangle and portions of adjacent quadrangles, 10 percent exceedance in 50 years peak ground acceleration—Predominant earthquake. .....57

Figure 3.5. Niles 7.5-Minute Quadrangle and portions of adjacent quadrangles, 10 percent exceedance in 50 years magnitude-weighted pseudo-peak acceleration for alluvium - Liquefaction opportunity .....58

Table 1.1. Correlation of Quaternary Stratigraphic Nomenclatures Used in Previous Studies.9

Table 1.2. Summary of Geotechnical Characteristics for Quaternary Geological Units in the Niles 7.5-Minute Quadrangle.....12

Table 1.3. Liquefaction susceptibility for Quaternary Map Units within the Niles 7.5-Minute Quadrangle .....13

Table 2.1. Summary of the Shear Strength Statistics for the Niles Quadrangle. .....40

Table 2.2. Summary of Shear Strength Groups for the Niles Quadrangle.....41

Table 2.3. Hazard Potential Matrix for Earthquake-Induced Landslides in the Niles Quadrangle.. .....44

Plate 1.1. Quaternary Geologic Map of the Niles 7.5-Minute Quadrangle, California, modified from J. Sowers (unpublished mapping). .....62

Plate 1.2. Depth to historically high ground water, and location of boreholes used in this study, Niles 7.5-Minute Quadrangle, California.....63

Plate 2.1. Landslide inventory, shear test sample locations, and areas of significant grading, Niles 7.5-Minute Quadrangle.....64

# EXECUTIVE SUMMARY

This report summarizes the methods and sources of information used to prepare the Seismic Hazard Zone Map for the Niles 7.5-Minute Quadrangle, Alameda County, California. The map displays the boundaries of zones of required investigation for liquefaction and earthquake-induced landslides over an area of approximately 60 square miles at a scale of 1 inch = 2,000 feet.

The southwestern part of the Niles Quadrangle consists of the gently sloping East Bay Plain east of San Francisco Bay. The rest of the area lies within the East Bay Hills, which rise to more than 2,500 feet at Mission Peak in the southeastern corner. Part of the city of Fremont covers the western half of the quadrangle. Parts of Newark, Union City, and Pleasanton also lie within the quadrangle. Much of the hilly terrain is unincorporated Alameda County land, including the community of Sunol. From Sunol Valley near the eastern border, Alameda Creek flows westward across the area within deeply incised Niles Canyon. Arroyo de la Laguna, the only outlet for the Livermore Basin to the east, joins Alameda Creek in Sunol Valley. Several smaller creeks also exit the hills and flow across the plain. Interstate Highways 880 and 680 cross the area and State Highway 84 follows Niles Canyon. Much of the lowlands has been developed for residential and commercial uses. Most of the steep terrain of the East Bay Hills is undeveloped and some of it is parkland, including Mission Peak Regional Park, Pleasanton Ridge Regional Park, Garin-Dry Creek Pioneer Regional Park and the Vargas Plateau.

The map was prepared by employing geographic information system (GIS) technology, which allows the manipulation of three-dimensional data. Information considered includes topography, surface and subsurface geology, borehole data, historical ground-water levels, existing landslide features, slope gradient, rock-strength measurements, geologic structure, and probabilistic earthquake shaking estimates. The shaking inputs are based upon probabilistic seismic hazard maps that depict peak ground acceleration, mode magnitude, and mode distance with a 10 percent probability of exceedance in 50 years.

The liquefaction zone is concentrated in the southwestern quarter and in the central part of the quadrangle between the Hayward Fault and the base of the hills south of the mouth of Niles Canyon. The combination of steep slopes in the dissected East Bay Hills and weak rocks has produced widespread and abundant landslides. These conditions contribute to an earthquake-induced landslide zone that covers about 36 percent of the quadrangle.

## How to view or obtain the map

Seismic Hazard Zone Maps, Seismic Hazard Zone Reports and additional information on seismic hazard zone mapping in California are available on the California Geological Survey's Internet page: http://www.consrv.ca.gov/CGS/index.htm

Paper copies of Official Seismic Hazard Zone Maps, released by CGS, which depict zones of required investigation for liquefaction and/or earthquake-induced landslides, are available for purchase from:

BPS Reprographic Services
149 Second Street
San Francisco, California 94105
(415) 512-6550

Seismic Hazard Zone Reports (SHZR) summarize the development of the hazard zone map for each area and contain background documentation for use by site investigators and local government reviewers. These reports are available for reference at CGS offices in Sacramento, San Francisco, and Los Angeles. **NOTE: The reports are not available through BPS Reprographic Services.**

# INTRODUCTION

The Seismic Hazards Mapping Act (the Act) of 1990 (Public Resources Code, Chapter 7.8, Division 2) directs the California Department of Conservation (DOC), Division of Mines and Geology (DMG) [now called California Geological Survey (CGS)] to delineate seismic hazard zones. The purpose of the Act is to reduce the threat to public health and safety and to minimize the loss of life and property by identifying and mitigating seismic hazards. City, county, and state agencies are directed to use the seismic hazard zone maps in their land-use planning and permitting processes. They must withhold development permits for a site within a zone until the geologic and soil conditions of the project site are investigated and appropriate mitigation measures, if any, are incorporated into development plans. The Act also requires sellers (and their agents) of real property within a mapped hazard zone to disclose at the time of sale that the property lies within such a zone. Evaluation and mitigation of seismic hazards are to be conducted under guidelines adopted by the California State Mining and Geology Board (SMGB) (DOC, 1997). The text of this report is on the Internet at http://gmw.consrv.ca.gov/shmp/SHMPsp117.asp

The Act directs SMGB to appoint and consult with the Seismic Hazards Mapping Act Advisory Committee (SHMAAC) in developing criteria for the preparation of the seismic hazard zone maps. SHMAAC consists of geologists, seismologists, civil and structural engineers, representatives of city and county governments, the state insurance commissioner and the insurance industry. In 1991, SMGB adopted initial criteria for delineating seismic hazard zones to promote uniform and effective statewide implementation of the Act. These initial criteria provide detailed standards for mapping regional liquefaction hazards. The Act also directed CGS to develop a set of probabilistic seismic maps for California and to research methods that might be appropriate for mapping earthquake-induced landslide hazards.

In 1996, working groups established by SHMAAC reviewed the prototype maps and the techniques used to create them. The reviews resulted in recommendations that 1) the process for zoning liquefaction hazards remain unchanged and 2) earthquake-induced landslide zones be delineated using a modified Newmark analysis.

This Seismic Hazard Zone Report summarizes the development of the hazard zone map. The process of zoning for liquefaction uses a combination of Quaternary geologic mapping, historical ground-water information, and subsurface geotechnical data. The process for zoning earthquake-induced landslides incorporates earthquake loading, existing landslide features, slope gradient, rock strength, and geologic structure. Probabilistic seismic hazard maps, which are the underpinning for delineating seismic hazard zones, have been prepared for peak ground acceleration, mode magnitude, and mode distance with a 10 percent probability of exceedance in 50 years (Petersen and others, 1996) in accordance with the mapping criteria.

This report summarizes seismic hazard zone mapping for potentially liquefiable soils and earthquake-induced landslides in the Niles 7.5-Minute Quadrangle.

# SECTION 1
# LIQUEFACTION EVALUATION REPORT

# Liquefaction Zones in the Niles 7.5-Minute Quadrangle, Alameda County, California

**By**
**Jacqueline D. J. Bott and Keith L. Knudsen**

**California Department of Conservation**
**California Geological Survey**

## PURPOSE

The Seismic Hazards Mapping Act (the Act) of 1990 (Public Resources Code, Chapter 7.8, Division 2) directs the California Department of Conservation (DOC), Division of Mines and Geology (DMG) [now called California Geological Survey (CGS)] to delineate Seismic Hazard Zones. The purpose of the Act is to reduce the threat to public health and safety and to minimize the loss of life and property by identifying and mitigating seismic hazards. Cities, counties, and state agencies are directed to use seismic hazard zone maps developed by CGS in their land-use planning and permitting processes. The Act requires that site-specific geotechnical investigations be performed prior to permitting most urban development projects within seismic hazard zones. Evaluation and mitigation of seismic hazards are to be conducted under guidelines adopted by the California State Mining and Geology Board (SMGB) (DOC, 1997). The text of this report is on the Internet at http://gmw.consrv.ca.gov/shmp/SHMPsp117.asp

Following the release of DMG Special Publication 117 (DOC, 1997), agencies in the Los Angeles metropolitan region sought more definitive guidance in the review of geotechnical investigations addressing liquefaction hazards. The agencies made their

request through the Geotechnical Engineering Group of the Los Angeles Section of the American Society of Civil Engineers (ASCE). This group convened an implementation committee under the auspices of the Southern California Earthquake Center (SCEC). The committee, which consisted of practicing geotechnical engineers and engineering geologists, released an overview of the practice of liquefaction analysis, evaluation, and mitigation techniques (SCEC, 1999). This text is also on the Internet at: http://www.scec.org/

This section of the evaluation report summarizes seismic hazard zone mapping for potentially liquefiable soils in the Niles 7.5-Minute Quadrangle. Section 2 (addressing earthquake-induced landslides) and Section 3 (addressing potential ground shaking) complete the report, which is one of a series that summarizes production of similar seismic hazard zone maps within the state (Smith, 1996). Additional information on seismic hazards zone mapping in California is on CGS's Internet web page: http://www.consrv.ca.gov/CGS/index.htm

## BACKGROUND

Liquefaction-induced ground failure historically has been a major cause of earthquake damage in northern California. During the 1989 Loma Prieta and 1906 San Francisco earthquakes, significant damage to roads, utility pipelines, buildings, and other structures in the San Francisco Bay area was caused by liquefaction-induced ground displacement.

Localities most susceptible to liquefaction-induced damage are underlain by loose, water-saturated, granular sediment within 50 feet of the ground surface. These geological and ground-water conditions are widespread in the San Francisco Bay Area, most notably in some densely populated valley regions and alluviated floodplains. In addition, the potential for strong earthquake ground shaking is high because of the many nearby active faults. The combination of these factors constitutes a significant seismic hazard, especially in areas marginal to the bay, including areas in the Niles Quadrangle.

## METHODS SUMMARY

Characterization of liquefaction hazard presented in this report requires preparation of maps that delineate areas underlain by potentially liquefiable sediment. The following were collected or generated for this evaluation:

- Existing geologic maps were used to provide an accurate representation of the spatial distribution of Quaternary deposits in the study area. Geologic units that generally are susceptible to liquefaction include late Quaternary alluvial and fluvial sedimentary deposits and artificial fill

- Ground-water maps constructed to show the historically highest known ground-water levels

- Geotechnical data analyzed to evaluate liquefaction potential of deposits

- Information on potential ground shaking intensity based on CGS probabilistic shaking maps

The data collected for this evaluation were processed into a series of geographic information system (GIS) layers using commercially available software. The liquefaction zone map was derived from a synthesis of these data and according to criteria adopted by the SMGB (DOC, 2000).

## SCOPE AND LIMITATIONS

Evaluation for potentially liquefiable soils generally is confined to areas covered by Quaternary (less than about 1.6 million years) sedimentary deposits. Such areas within the Niles Quadrangle consist mainly of low-lying shoreline regions, alluviated valleys, floodplains, and canyons. CGS's liquefaction hazard evaluations are based on information on earthquake ground shaking, surface and subsurface lithology, geotechnical soil properties, and ground-water depth, which is gathered from various sources. Although selection of data used in this evaluation was rigorous, the quality of the data used varies. The State of California and the Department of Conservation make no representations or warranties regarding the accuracy of the data obtained from outside sources.

Liquefaction zone maps are intended to prompt more detailed, site-specific geotechnical investigations, as required by the Act. As such, liquefaction zone maps identify areas where the potential for liquefaction is relatively high. They do not predict the amount or direction of liquefaction-related ground displacements, or the amount of damage to facilities that may result from liquefaction. Factors that control liquefaction-induced ground failure are the extent, depth, density, and thickness of liquefiable materials, depth to ground water, rate of drainage, slope gradient, proximity to free faces, and intensity and duration of ground shaking. These factors must be evaluated on a site-specific basis to assess the potential for ground failure at any given project site.

Information developed in the study is presented in two parts: physiographic, geologic, and hydrologic conditions in PART I, and liquefaction and zoning evaluations in PART II.

# PART I

## PHYSIOGRAPHY

### Study Area Location and Physiography

The Niles 7.5-Minute Quadrangle covers approximately 60 square miles in Alameda County. The quadrangle is mostly comprised of the city of Fremont and unincorporated Alameda County, which includes the town of Sunol in Sunol Valley. Other cities whose

boundaries extend into the quadrangle include Newark and Union City, the majority of which are located within the adjacent Newark Quadrangle to the west. Also a small part of the city of Pleasanton extends into the northeastern corner of the Niles Quadrangle.

The southwestern part of the Niles Quadrangle consists of the gently sloping East Bay Plain east of San Francisco Bay. The rest of the area lies within the East Bay Hills. The northern end of Sunol Valley, a narrow, northwest-trending, linear, flat-bottomed valley on the eastern side of the quadrangle, provides a break in the hills. Elevations rise from less than 10 feet above sea level in the southwestern corner of the quadrangle, to 2,517 feet at the summit of Mission Peak, in the southeastern corner. The prominent northwest-trending ridges within the East Bay Hills are mostly above 1,200 feet, with Sunol Ridge, northwest of Sunol, at over 2,000 feet. Alameda Creek flows northwestwards through Sunol Valley and meets Arroyo de la Laguna at the head of Niles Canyon. Arroyo de la Laguna is the only outlet for the Livermore Basin that is located northeast of the Niles Quadrangle. Alameda Creek crosses the East Bay Hills through steep-sided Niles Canyon and then flows westward across the East Bay Plain towards San Francisco Bay along a man-made channel that is locally concrete-lined. There are several smaller tributary drainages to Alameda Creek and Arroyo de la Laguna in this area, one of the largest being Sinbad Creek. Several small creeks flow out of the East Bay Hills and directly onto the East Bay Plain, including Mission Creek and Agua Caliente Creek.

There are two Interstate Highways in the map area. Interstate 880 crosses northwesterly through the southwestern corner of the quadrangle and Interstate 680 follows along the base of the East Bay Hills from the south, and then turns northeastwards and crosses the hills to Sunol Valley south of Niles Canyon. Highway 84 follows Alameda Creek along Niles Canyon and Highway 238 follows the western edge of the East Bay Hills. The Bay Area Rapid Transit Fremont Line terminates in central Fremont and both Western Pacific and Southern Pacific railroads pass through the quadrangle. The Hetch-Hetchy Aqueduct crosses the center of the quadrangle.

Most of the gently sloping alluvial plains within the Niles Quadrangle have been developed for residential and commercial uses. Most of the steeply sloping East Bay Hills are undeveloped and there are several parks in the hills. Land in and around flat-bottomed Sunol Valley is owned by the San Francisco Water District and has been utilized for gravel quarrying and agriculture. Some large abandoned gravel quarries, just north of the Alameda Creek channel in Fremont, have been developed as the Quarry Lakes Regional Recreation Area and are used as percolation ponds utilizing water diverted from Alameda Creek to replenish the underlying aquifers. Parts of the Mission Peak Regional Park, the Pleasanton Ridge Regional Park, the Garin-Dry Creek Pioneer Regional Park and the newly acquired Vargas Plateau, all managed by the East Bay Regional Park District, are within this quadrangle.

# GEOLOGY

## Bedrock and Surficial Geology

Geologic units that generally are susceptible to liquefaction include late Quaternary alluvial and fluvial sedimentary deposits and artificial fill. To evaluate the areal distribution of Quaternary deposits in the Niles Quadrangle, bedrock mapping by Graymer and others (1996) was obtained from the U.S. Geological Survey in digital form and merged with unpublished mapping of Quaternary deposits by J.M. Sowers of William Lettis & Associates, Inc. These GIS maps were combined, with some modifications along the bedrock/Quaternary contact and to the Quaternary mapping along the Arroyo de la Laguna and the Alameda Creek in Sunol Valley, to form a single, 1:24,000-scale geologic map of the Niles Quadrangle (Plate 1.1). Modifications to the mapping of Quaternary deposits were based on 2002 aerial photographs, 1993 Digital Orthophoto Quadrangles and limited field reconnaissance. The distribution of Quaternary deposits on this map (summarized on Plate 1.1) was used in combination with other data, discussed below, to evaluate liquefaction susceptibility and develop the Liquefaction Zone of Required Investigation.

Other geologic maps and reports were reviewed, including Clark (1915), Trask and Rolston (1951), Radbruch (1959), Goldman (1969), DWR (1966), DWR (1967), DWR (1968), DWR (1974), DWR (1975), Atwater and others (1977), Helley and others (1979), Borchardt (1988), Barlock (1989), Bull (1991), Sloan and Aubrey (1991), Rogers and Figuers (1992), Lienkaemper (1992), Sloan (1992), Koltermann and Gorelick (1992), Kelson and others (1993), Luhdorff and Scalmanini Consulting Engineers (1993), Koltermann (1994), Helley and Graymer (1997), Knudsen and others (2000), Treadwell & Rollo, Inc. (2001), Collins (2001), and Lienkaemper and others (2002). Limited field reconnaissance was conducted to confirm the location of geologic contacts, observe properties of near-surface deposits, and characterize the surface expression of individual geologic units.

In the Niles Quadrangle, Sowers (unpublished mapping) identified 23 Quaternary map units (Plate 1.1). The Quaternary geologic mapping methods used by Sowers (unpublished mapping) in the Niles Quadrangle are the same as those described by Knudsen and others (2000), which consist of interpretation of topographic maps, aerial photographs, and soil surveys, as well as compiled published and unpublished geologic maps. The authors estimate the ages of deposits using: landform shape, relative geomorphic position, cross cutting relationships, superposition, depth and degree of surface dissection, and relative degree of soil profile development. Table 1.1 compares stratigraphic nomenclature used in Knudsen and others (2000) and the CGS GIS database, with that of several previous maps.

| UNIT | Knudsen and others (2000) Sowers (unpublished) | Helley and Graymer (1997) | Helley and others (1979) | CGS GIS database |
|---|---|---|---|---|
| artificial fill | af | af | | af |
| gravel quarries and percolation ponds | gq | GP | | gq |
| artificial levee fill | alf | alf | | alf |
| artificial stream channel | ac | Qhasc | | ac |
| modern stream channel deposits | Qhc | Qhsc | Qhsc | Qhc |
| latest Holocene alluvium undifferentiated | Qhay | | | Qhay |
| latest Holocene alluvial fan levee deposits | Qhly | | | Qhly |
| latest Holocene stream terrace deposits | Qhty | Qhfpl1, Qhfpl2 | | Qhty |
| Holocene San Francisco Bay mud | Qhbm | Qhbm | Qhbm | Qhbm |
| Holocene basin deposits | Qhb | Qhb, Qhbs | | Qhb |
| Holocene alluvial fan deposits | Qhf, Qhf1, Qhf2 | Qhaf | Qham, Qhfp | Qhf |
| Holocene alluvial fan deposits, fine grained facies | Qhff | | Qhaf | Qhff |
| Holocene alluvial fan levee deposits | Qhl | Qhl | | Qhl |
| Holocene stream terrace deposits | Qht | Qhfp | | Qht |
| Holocene alluvium, undifferentiated | Qha | Qhaf | | Qha |
| latest Pleistocene to Holocene alluvial fan deposits | Qf | | | Qf |
| latest Pleistocene to Holocene alluvial fan levee deposits | Ql | | | Ql |
| latest Pleistocene to Holocene stream terrace deposits | Qt | | | Qt |
| latest Pleistocene to Holocene alluvium, undifferentiated | Qa | | | Qa |

| | | | | |
|---|---|---|---|---|
| latest Pleistocene stream terrace deposits | Qpt | | | Qpt |
| latest Pleistocene alluvial fan deposits | Qpf | Qpaf | | Qpf |
| early to middle Pleistocene alluvial fan deposits | Qof | Qpaf, Qpoaf | | Qof |
| early to middle Pleistocene stream terrace deposits | Qot | | | Qot |
| early to middle Pleistocene undifferentiated alluvial deposits | Qoa | Qpaf, Qpoaf | Qpea, Qpmc | Qoa |
| bedrock | br | br | | br |

**Table 1.1. Correlation of Quaternary Stratigraphic Nomenclatures Used in Previous Studies**. For this study, CGS has adopted the nomenclature of Knudsen and others (2000).

The gentle southwest-sloping alluvial plane within the Niles Quadrangle is covered by Holocene or latest Pleistocene to early Holocene alluvial fan and associated deposits (Sowers, unpublished mapping), most of which been deposited by Alameda Creek. Alameda Creek, which crosses the East Bay Hills, has a large watershed that covers an area of approximately 630 square miles and includes all tributaries of Arroyo de la Laguna, the only outflow from the Livermore basin. Holocene and Pleistocene alluvial and fluvial deposits have been mapped in the Sunol Valley and terraces of early Pleistocene to Holocene age have been mapped along Niles Canyon. Undifferentiated latest Pleistocene to Holocene alluvium (Qa) has been mapped in many upland valley areas. A small amount of Holocene Bay Mud (Qhbm) is exposed in the very southwestern corner of the quadrangle. Rocks of Cretaceous to Plio-Pleistocene age are exposed in the hilly terrain in the northeastern two thirds of the map area.

The Holocene alluvial fan deposits have been subdivided into the following units by Sowers (unpublished mapping): Qhc, Qhly, Qhty, Qht, Qhf, Qhff, Qhb, Qha, and Qhay (Plate 1.1). Active stream-channel deposits (Qhc) are mapped along the beds of Alameda Creek, Mission Creek and Arroyo de La Laguna. Latest Holocene levee deposits (Qhly) are only mapped on the north side of Alameda Creek in Fremont. Latest Holocene stream terrace deposits (Qhty) are mapped along Alameda Creek, mainly below Niles Canyon. Latest Holocene stream terrace deposits also have been mapped in places along Arroyo de La Laguna. Holocene terrace deposits (Qht) are mapped flanking both Alameda Creek and Arroyo de La Laguna. Sowers (unpublished mapping) mapped some areas of undivided Holocene alluvial fan deposits (Qhf) and two geomorphically distinct subsets of these (Qhf1 and Qhf2) within the Alameda Creek fan. Fine-grained fan deposits (Qhff) are mapped at the distal part of the Alameda Creek fan, and along the

lower reaches of Mission Creek. Fine-grained fan deposits also have been mapped east of the Holocene basin deposits (Qhb) that are mapped around man-made Lake Elizabeth in Fremont Central Park. The presence of basin deposits indicates natural ponding has occurred in this area. The ponding is probably controlled by vertical displacement along the Hayward Fault, which also acts as a ground-water barrier (see section on Ground Water). Holocene alluvium has been mapped along the Holocene channel (Qha) of Vallecitos Creek, a tributary to Arroyo de La Laguna and in a few places along Alameda Creek and alluvial fan. A small area at the confluence of Vallecitos Creek and Arroyo de La Laguna has been mapped as undifferentiated latest Holocene alluvial deposits (Qhay).

A large part of the southern portion of the Alameda Creek alluvial fan (also known as the Niles cone) is mapped as latest Pleistocene to Holocene alluvial fan deposits (Qf). However, this area is underlain by a varying thickness of Holocene deposits, based on the interpretation of subsurface geotechnical data. These Holocene deposits, based on geomorphic relationships, are older than Qhf1 and Qhf2. Areas along Mission Creek and along the foot of the East Bay Hills south of where Mission Creek turns toward the south, also are mapped as latest Pleistocene to Holocene alluvial fan deposits (Qf), but these appear to be mostly Pleistocene in age based on the interpretation of subsurface geotechnical data. Latest Pleistocene to Holocene alluvial fan levee deposits (Ql) are mapped by Sowers (unpublished mapping) across the Niles cone. Again, based on interpretation of subsurface geotechnical data, these deposits are thought to be Holocene.

Latest Pleistocene alluvial fan deposits (Qpf) have been mapped south of Mission Creek, along the Hayward Fault and also in some upland valleys southwest of Sunol Valley. Latest Pleistocene alluvial fan deposits also have been interpreted within the subsurface. A few remnants of latest Pleistocene stream terrace deposits (Qpt) are mapped along Alameda Creek in Niles Canyon and Sunol Valley. Sowers (unpublished mapping) mapped a small area of what is thought to be early to late Pleistocene alluvial fan deposits (Qoa) south of Mission Creek, and also within an upland valley towards the center of the quadrangle. Early to late Pleistocene undifferentiated alluvial fan deposits (Qof) are mapped within an upland valley southwest of Sunol Valley. A few isolated outcrops of early to late Pleistocene stream terrace deposits (Qot) have been mapped along Alameda Creek in Niles Canyon and Sunol Valley.

Graymer and others (1996) mapped Tertiary to Quaternary Livermore and Irvington gravels (QTl and QTi) in this quadrangle. Other bedrock exposed in the northeastern two thirds of the Niles 7.5-Minute Quadrangle includes: Tertiary sedimentary and volcanic rocks (Tbr, TccsI, Tcs, To, Tor, Tord, Tpsu, Tr, Tshs, Tssc, Tsso, Tt, Ttls, Ttss and Tv), Late Jurassic and /or Early Cretaceous Franciscan melange (fm), and Mesozoic sedimentary rocks of the Great Valley sequence (KJK, KJkc, Kc, Kcv, Ko, Kp, Kr, KsVII, and KuII) (Graymer and others, 1996). See the eEarthquake-induced landslide portion (Section 2) of this report for further description of the bedrock geology.

**Structural Geology**

The Niles Quadrangle is within the active San Andreas Fault system, which distributes shearing across a complex system of primarily northwest-trending, right-lateral, strike-

slip faults that include the San Andreas, Hayward, and Calaveras faults. The Hayward Fault passes diagonally through the southwestern part of the Niles Quadrangle and the Calaveras Fault passes through its northeastern corner (Plate 1.1).

## ENGINEERING GEOLOGY

Information on subsurface geology and engineering characteristics of flatland deposits was obtained from borehole logs collected from reports on geotechnical and environmental projects. For this investigation, about 120 borehole logs were collected from the files of the city of Fremont, city of Newark, Alameda County, San Francisco Public Utilities Commission, Harlan Tait Associates (1995) and Caltrans. Data from 110 borehole logs were entered into a CGS geotechnical GIS database (Table 1.2). Boreholes from gravel quarries in the Sunol Valley (Treadwell & Rollo, Inc., 2001) were used to evaluate the subsurface geologic materials qualitatively. These boreholes were drilled with a Becker Hammer drill rig with an open crowd-in bit, so blow counts were not easily converted to SPT-equivalent blow counts for liquefaction analysis.

Standard Penetration Tests (SPTs) provide a standardized measure of the penetration resistance of geologic deposits and are commonly used as an index of soil density. This in-field test consists of counting the number of blows required to drive a split-spoon sampler (1.375-inch inside diameter) one foot into the soil at the bottom of a borehole at chosen intervals while drilling. The driving force is provided by dropping a 140-pound hammer weight 30 inches. The SPT method is formally defined and specified by the American Society for Testing and Materials in test method D1586 (ASTM, 1999). Recorded blow counts for non-SPT geotechnical sampling where the sampler diameter, hammer weight or drop distance differ from those specified for an SPT (ASTM D1586), are converted to SPT-equivalent blow counts. The actual and converted SPT blow counts are normalized to a common-reference, effective-overburden pressure of one atmosphere (approximately one ton per square foot) and a hammer efficiency of 60 percent using a method described by Seed and Idriss (1982) and Seed and others (1985). This normalized blow count is referred to as $(N_1)_{60}$.

As stated above, geotechnical and environmental borehole logs provide information on lithologic and engineering characteristics of Quaternary deposits. Geotechnical characteristics of the Quaternary map units are summarized in Table 1.2 and their composition by soil type is presented in Table 1.3. These tables reveal that: 1) Holocene materials generally are less dense and more readily penetrated than Pleistocene materials; 2) latest Pleistocene alluvial fan deposits (Qpf) have higher dry density and much higher penetration resistance than Holocene alluvial fan deposits (Qhf); 3) latest Pleistocene alluvial fan deposits (Qpf) contain more gravel and are coarser than Holocene alluvial fan deposits (Qhf); 4) Holocene alluvial fan deposits are predominantly fine grained, but have silt and silty sand lenses that have the potential to liquefy; and 5) dry density and penetration resistance values for most units have a large variability.

| GEOLOGIC MAP UNIT | | DRY DENSITY (pounds per cubic foot) | | | | | | STANDARD PENETRATION RESISTANCE (blows per foot, $(N_1)_{60}$) | | | | | |
|---|---|---|---|---|---|---|---|---|---|---|---|---|---|
| Unit (1) | Texture (2) | Number of Tests | Mean | C (3) | Median | Min | Max | Number of Tests | Mean | C (3) | Median | Min | Max |
| **af** | Fine | 8 | 110.2 | 0.12 | 115.5 | 90.3 | 124.0 | 14 | 56 | 0.67 | 44 | 9 | >99 |
| | Coarse | 4 | 126.5 | 0.05 | 126.5 | 121.0 | 132.0 | 19 | 44 | 0.84 | 39 | 5 | >99 |
| **Qhly** | Fine | 3 | 98.3 | 0.03 | 97.0 | 96.0 | 102.0 | 2 | 21 | 0.05 | 21 | 20 | 22 |
| | Coarse | 0 | - | - | - | - | - | 0 | - | - | - | - | - |
| **Qhb** | Fine | 10 | 93.1 | 0.12 | 90.5 | 74.0 | 107.0 | 18 | 9 | 0.44 | 9 | 2 | 18 |
| | Coarse | 0 | - | - | - | - | - | 0 | - | - | - | - | - |
| **Qhf** | Fine | 68 | 103.3 | 0.09 | 104.0 | 84.0 | 125.5 | 140 | 14 | 0.68 | 12 | 1 | 72 |
| | Coarse | 30 | 102.9 | 0.08 | 103.3 | 89.0 | 117.0 | 73 | 13 | 0.64 | 11 | 4 | 45 |
| **Qhff** | Fine | 3 | 89.0 | 0.22 | 83.0 | 73.0 | 111.0 | 3 | 18 | 0.40 | 14 | 13 | 26 |
| | Coarse | 2 | 107.5 | 0.06 | 107.5 | 103.0 | 112.0 | 1 | 10 | - | - | - | - |
| **Qhl** | Fine | 2 | 106.0 | 0.08 | 106.0 | 100.0 | 112.0 | 2 | 7 | 0.28 | 7 | 6 | 9 |
| | Coarse | 0 | - | - | - | - | - | 0 | - | - | - | - | - |
| **Qha** | Fine | 4 | 107.4 | 0.04 | 106.5 | 103.0 | 113.7 | 6 | 21 | 0.68 | 15 | 9 | 47 |
| | Coarse | 0 | - | - | - | - | - | 0 | - | - | - | - | - |
| **Qf** | Fine | 11 | 106.9 | 0.05 | 107.0 | 99.0 | 115.0 | 27 | 14 | 0.49 | 14 | 4 | 32 |
| | Coarse | 5 | 108.8 | 0.14 | 104.0 | 92.0 | 130.0 | 44 | 18 | 0.87 | 14 | 5 | 90 |
| **Qpf** | Fine | 51 | 107.6 | 0.07 | 108.0 | 84.0 | 123.2 | 96 | 26 | 0.68 | 20 | 4 | 97 |
| | Coarse | 23 | 119.0 | 0.10 | 116.2 | 99.0 | 137.0 | 137 | 39 | 0.61 | 32 | 10 | >99 |

Notes:
(1) See Table 1.3 for names of the units listed here.
(2) Fine soils (silt and clay) contain a greater percentage passing the #200 sieve (<.074 mm); coarse soils (sand and gravel) contain a greater percentage not passing the #200 sieve.
(3) C = coefficient of variation (standard deviation divided by the mean)

## Table 1.2. Summary of Geotechnical Characteristics for Quaternary Geological Units in the Niles 7.5-Minute Quadrangle.

| Geologic Unit (1) | Description | Total Layer Thickness (ft) | Composition by Soil Type (Unified Soil Classification System Symbols) | Depth to ground water (ft) (2) and liquefaction susceptibility category assigned to geologic unit | | | |
|---|---|---|---|---|---|---|---|
| | | | | <10 | 10 to 30 | 30 to 40 | >40 |
| **af** | Artificial fill (3) | 211 | CL 24%; SM 23% GW 21%; Other 32% | VH - L | H - L | M - L | VL |
| **alf** | Artificial levee fill | - | - | VH-L | H-L | M-L | VL |
| **ac** | Artificial channel | - | - | VH | H | M | VL |
| **Qhc** | Modern stream channel deposits | - | - | VH | H | M | VL |
| **Qhay** | Latest Holocene alluvium undifferentiated | - | - | H | H | M | VL |
| **Qhly** | Latest Holocene alluvial fan levee deposits | 16 | ML 100% | VH | H | M | VL |

| | | | | | | | |
|---|---|---|---|---|---|---|---|
| **Qhty** | Latest Holocene stream terrace deposits | - | - | H | H | M | VL |
| **Qhbm** | Holocene San Francisco Bay mud | - | - | H | M | L | VL |
| **Qhb** | Holocene basin deposits | 160 | CH 36%; CL 32%<br>ML 28%; Other 4% | M | M | L | VL |
| **Qhf** | Holocene alluvial fan deposits | 1294 | CL 30%; ML 30%<br>SM 20%; Other 20% | H | M | L | VL |
| **Qhff** | Holocene alluvial fan deposits, fine grained facies | 47 | CL 51%; ML 25%<br>CH 15%; Other 9% | M | M | L | VL |
| **Qhl** | Holocene alluvial fan levee deposits | 17 | ML 57%; CL 43% | H | M | L | VL |
| **Qht** | Holocene stream terrace deposits | - | - | H | M | L | VL |
| **Qha** | Holocene alluvium, undifferentiated | 32 | CL 52%; ML 26%<br>CH 22% | M | M | L | VL |
| **Qf** | Latest Pleistocene to Holocene alluvial fan deposits | 486 | CL 24%; SM 18%<br>SP 16%; ML 16%<br>Other 26% | M | L | L | VL |
| **Ql** | Latest Pleistocene to Holocene alluvial fan levee deposits | - | - | M | L | L | VL |
| **Qt** | Latest Pleistocene to Holocene stream terrace deposits | - | - | M | L | L | VL |
| **Qa** | Latest Pleistocene to Holocene alluvium, undifferentiated | - | - | M | L | L | VL |
| **Qpt** | Latest Pleistocene stream terrace deposits | - | - | L | L | VL | VL |
| **Qpf** | Latest Pleistocene alluvial fan deposits | 2182 | CL 24%; GW 20%; SM 15%<br>SW 10%; Other 31% | L | L | VL | VL |
| **Qof** | Early to middle Pleistocene alluvial fan deposits | - | - | L | L | VL | VL |
| **Qot** | Early to middle Pleistocene stream terrace deposits | - | - | L | L | VL | VL |
| **Qoa** | Early to middle Pleistocene undifferentiated alluvial deposits | - | - | L | L | VL | VL |
| **B** | Bedrock | n/a | n/a (4) | VL | VL | VL | VL |

Notes:
(1) Susceptibility assignments are specific to the materials within the Niles 7.5-Minute Quadrangle.
(2) Based on the Simplified Procedure (Seed and Idriss, 1971; Youd and Idriss, 1997) and a small number of borehole analyses for some units.
(3) The liquefaction susceptibility of artificial fill ranges widely, depending largely on the nature of the fill, its age, and whether it was compacted during emplacement.
(4) n/a = not applicable

**Table 1.3. Liquefaction Susceptibility for Quaternary Map Units Within the Niles 7.5-Minute Quadrangle.** Units indicate relative susceptibility of deposits to liquefaction as a function of material type and ground water depth within that deposit. VH = very high, H = high, M = moderate, L = low, and VL = very low to none.

## GROUND WATER

Liquefaction hazard may exist in areas where depth to ground water is 40 feet or less. CGS uses the highest known ground-water levels because water levels during a future earthquake cannot be anticipated because of the unpredictable fluctuations caused by natural processes and human activities. A historical-high ground-water map differs from most ground-water maps, which show the actual water levels at a particular time. Plate 1.2 depicts a hypothetical ground-water level within alluviated areas.

Ground-water conditions were investigated in the Niles Quadrangle to evaluate the depth to saturated materials. Saturated conditions reduce the effective normal stress, thereby increasing the likelihood of earthquake-induced liquefaction (Youd, 1973). The evaluation was based on first-encountered water noted in geotechnical borehole logs acquired from the city of Fremont, the Regional Water Quality Control Board, Alameda County, San Francisco Public Utilities Commission, Harlan Tait Associates and the city of Newark. The depths to first-encountered unconfined ground water were plotted onto a map of the project area to constrain the estimate of historically shallowest ground water. Water depths from boreholes known to penetrate confined aquifers were not utilized. A ground-water map constructed by Clark (1915) for the1913-1914 season was used to develop historically high ground-water contours to the east of the Hayward Fault as we obtained few recent ground-water measurements in this region.

Regional ground-water contours on Plate 1.2 show historical-high water depths, as interpreted from the above data sources and from boring logs from investigations between 1959 and 1999. Depths to first-encountered water range from 2 to 59 feet below the ground surface, although most of the East Bay alluvial plain has ground-water levels within 40 feet of the ground surface. The Hayward Fault acts as a ground-water barrier (Clark, 1915) and separates two areas with different ground-water levels. Very shallow ground water occurs east of the Hayward Fault near the lake in Fremont Central Park and also Tule Pond, but is more than 40 feet below the ground surface west of the Hayward Fault (Plate 1.2).

Pumping of ground water for irrigation, which began in the 1920's, depleted the uppermost Newark aquifer of the Niles cone west of the Hayward Fault, resulting in salt-water intrusion into the aquifer (DWR, 1968). Subsequent pumping of water from the lower Centerville aquifer (separated from the Newark aquifer by a thick clay layer), which was thought to relieve the upper aquifer problems, caused salt-water contamination in the lower aquifer by 1950. DWR (1968) reports that pumping in the lower aquifer caused a hydraulic gradient that drew saline water landward within the upper Newark aquifer then down into the Centerville aquifer close to the Hayward Fault where the two aquifers are inferred to be connected. Recharge of ground water to restore the quality of the aquifer is being accomplished through percolation of diverted water from Alameda Creek into some abandoned gravel quarry pits at what is now the Quarry Lakes Regional Preserve. Also, the Alameda County Water District pumps the saline water from the contaminated aquifers and either desalinates the water or empties it into the San Francisco Bay. DWR (1968) reports that ground-water levels west of the Hayward Fault had been at or below sea level from about 1913 until the mid 1960's due to pumping but

the ground-water surface sloped toward the bay before this time. Current ground-water levels west of the Hayward Fault are similar to those shown by Clark (1915) for the 1913-1914 season.

Only a few ground-water measurements were available for the Sunol Valley from geotechnical boreholes and the Regional Water Quality Control Board, but additional information about the ground water in this area was obtained from reports by Scalmanini and Luhdorff Consulting Engineers (1993), Treadwell & Rollo, Inc (2001) and Collins (2001). Geotechnical boreholes just south of Arroyo de la Laguna in Sunol Valley show ground water at about 20 feet below the terrace surface (Qht) (Plate 1.2). Scalmanini and Luhdorff Consulting Engineers (1993), in their study of ground-water resources of Sunol Valley for the San Francisco Water Department, conclude based on the limited ground-water measurements since 1986, that depth to shallow ground water is typically in the range of 20 to 30 feet in Sunol Valley. Ground-water seepage at this approximate depth was noted during field reconnaissance in one of the Mission Valley Rock quarries in Sunol Valley south of I680. However, water-level measurements in boreholes drilled for Mission Valley Rock (Treadwell & Rollo, Inc., 2001) over a number of years indicate a large variation in ground-water levels, and in 2001 depths to ground water were greater than 100 feet in some areas. Based on logs of deep boreholes (Treadwell & Rollo, Inc., 2001) there appear to be numerous discontinuous aquifers and aquitards within the alluvium in Sunol Valley. Scalmanini and Luhdorff Consulting Engineers (1993) conclude that alluvium below about 40 feet (interpreted by them to be Livermore Gravels) has a much lower porosity and is less useful for ground-water storage in comparison to the younger upper alluvium, based on pump tests. Therefore, the upper alluvium appears to contain perched water and we interpret the ground water to be at depths of about 20 to 30 feet below the ground surface.

## PART II

## LIQUEFACTION POTENTIAL

Liquefaction may occur in water-saturated sediment during moderate to great earthquakes. Liquefied sediment loses strength and may fail, causing damage to buildings, bridges, and other structures. Many methods for mapping liquefaction hazard have been proposed. Youd (1991) highlights the principal developments and notes some of the widely used criteria. Youd and Perkins (1978) demonstrate the use of geologic criteria as a qualitative characterization of liquefaction susceptibility and introduce the mapping technique of combining a liquefaction susceptibility map and a liquefaction opportunity map to produce a liquefaction potential map. Liquefaction susceptibility is a function of the capacity of sediment to resist liquefaction. Liquefaction opportunity is a function of the potential seismic ground shaking intensity.

The method applied in this study for evaluating liquefaction potential is similar to that of Tinsley and others (1985). Tinsley and others (1985) applied a combination of the techniques used by Seed and others (1983) and Youd and Perkins (1978) for their

mapping of liquefaction hazards in the Los Angeles region. CGS's method combines geotechnical analyses, geologic and hydrologic mapping, and probabilistic earthquake shaking estimates, but follows criteria adopted by the SMGB (DOC, 2000).

## LIQUEFACTION SUSCEPTIBILITY

Liquefaction susceptibility reflects the relative resistance of a soil to loss of strength when subjected to ground shaking. Physical properties of soil such as sediment grain-size distribution, compaction, cementation, saturation, and depth govern the degree of resistance to liquefaction. Some of these properties can be correlated to a sediment's geologic age and environment of deposition. With increasing age, relative density may increase through cementation of the particles or compaction caused by the weight of the overlying sediment. Grain-size characteristics of a soil also influence susceptibility to liquefaction. Sand is more susceptible than silt or gravel, although silt of low plasticity is treated as liquefiable in this investigation. Cohesive soils generally are not considered susceptible to liquefaction. Such soils may be vulnerable to strength loss with remolding and represent a hazard that is not addressed in this investigation. Soil characteristics and processes that result in higher measured penetration resistances generally indicate lower liquefaction susceptibility. Thus, blow count and cone penetrometer values are useful indicators of liquefaction susceptibility.

Saturation is required for liquefaction, and the liquefaction susceptibility of a soil varies with the depth to ground water. Very shallow ground water increases the susceptibility to liquefaction (soil is more likely to liquefy). Soils that lack resistance (susceptible soils) typically are saturated, loose and sandy. Soils resistant to liquefaction include all soil types that are dry, cohesive, or sufficiently dense.

CGS's map inventory of areas containing soils susceptible to liquefaction begins with evaluation of geologic maps and historical occurrences, cross-sections, geotechnical test data, geomorphology, and ground-water hydrology. Soil properties and soil conditions such as type, age, texture, color, and consistency, along with historical depths to ground water are used to identify, characterize, and correlate susceptible soils. Because Quaternary geologic mapping is based on similar soil observations, liquefaction susceptibility maps typically are similar to Quaternary geologic maps. CGS's qualitative relations among susceptibility, geologic map unit and depth to ground water are summarized in Table 1.3.

Most Holocene materials where water levels are within 30 feet of the ground surface have susceptibility assignments of high (H) to very high (VH) (Table 1.3) including uncompacted fill and fill levee deposits. Holocene basin deposits (Qhb), Holocene alluvial fan fine facies deposits (Qhff), and undifferentiated Holocene alluvium (Qha) primarily are composed of fine-grained material and have correspondingly lower susceptibility assignments. However, these units may contain lenses of material with higher liquefaction susceptibility. Latest Pleistocene to Holocene alluvial fan deposits within 30 feet of the ground surface have moderate (M) to low (L) susceptibility assignment as they have lower average blow counts than Latest Pleistocene deposits and

may contain lenses of potentially liquefiable material (Table 1.3). Other latest Pleistocene to Holocene deposits have been given the same susceptibility assignments. All latest Pleistocene and older deposits within 30 feet of the ground surface have low (L) susceptibility assignments based on higher densities and blow counts. Uncompacted artificial fill and all latest Holocene deposits have moderate (M) susceptibility assignments where they are saturated between 30 and 40 feet. All other units have low (L) to (VL) susceptibility assignments below 30 feet of the ground surface.

## LIQUEFACTION OPPORTUNITY

Liquefaction opportunity is a measure, expressed in probabilistic terms, of the potential for strong ground shaking. Analyses of in-situ liquefaction resistance require assessment of liquefaction opportunity. The minimum level of seismic excitation to be used for such purposes is the level of peak ground acceleration (PGA) with a 10 percent probability of exceedance over a 50-year period (DOC, 2000). The earthquake magnitude used in CGS's analysis is the magnitude that contributes most to the calculated PGA for an area.

For the Niles Quadrangle, PGAs of 0.59-0.88g, resulting from earthquakes of magnitude 6.8 to 7.1 were used for liquefaction analyses. The PGA and magnitude values were based on de-aggregation of the probabilistic hazard at the 10 percent in 50-year hazard level (Petersen and others, 1996). See section 3 of this report for additional description of ground motions.

### Quantitative Liquefaction Analysis

CGS performs quantitative analysis of geotechnical data to evaluate liquefaction potential using the Seed-Idriss Simplified Procedure (Seed and Idriss, 1971; Seed and others, 1983; National Research Council, 1985; Seed and others, 1985; Seed and Harder, 1990; Youd and Idriss, 1997; Youd and others, 2001). Using the Seed-Idriss Simplified Procedure one can calculate soil resistance to liquefaction, expressed in terms of cyclic resistance ratio (CRR), based on SPT results, ground-water level, soil density, moisture content, soil type, and sample depth. CRR values are then compared to calculated earthquake-generated shear stresses expressed in terms of cyclic stress ratio (CSR). The Seed-Idriss Simplified Procedure requires normalizing earthquake loading relative to a M7.5 event for the liquefaction analysis. To accomplish this, CGS's analysis uses the Idriss magnitude-scaling factor (MSF) (Youd and Idriss, 1997). It is convenient to think in terms of a factor of safety (FS) relative to liquefaction, where: FS = (CRR / CSR) * MSF. FS, therefore, is a quantitative measure of liquefaction potential. CGS uses a factor of safety of 1.0 or less, where CSR equals or exceeds CRR, to indicate the presence of potentially liquefiable soil. While an FS of 1.0 is considered the "trigger" for liquefaction, for a site specific analysis an FS of as much as 1.5 may be appropriate depending on the vulnerability of the site and related structures.

The CGS liquefaction analysis program calculates an FS for each geotechnical sample where blow counts were collected. Typically, multiple samples are collected for each borehole. The program then independently calculates an FS for each non-clay layer that includes at least one penetration test using the minimum $(N_1)_{60}$ value for that layer. The

minimum FS value of the layers penetrated by the borehole is used to determine the liquefaction potential for each borehole location. The reliability of FS values varies according to the quality of the geotechnical data. FS, as well as other considerations such as slope, presence of free faces, and thickness and depth of potentially liquefiable soil, are evaluated in order to construct liquefaction potential maps, which are then used to make a map showing zones of required investigation.

Of the 110 geotechnical and environmental borehole logs reviewed in this study (Plate 1.2) 92 include blow-count data from SPTs or from penetration tests that allow reasonable blow count translations to SPT-equivalent values. Non-SPT values, such as those resulting from the use of 2-inch or 2½-inch inside-diameter ring samplers, were translated to SPT-equivalent values if reasonable factors could be used in conversion calculations. The reliability of the SPT-equivalent values varies. Therefore, they are weighted and used in a more qualitative manner. Few borehole logs, however, include all of the information (for example, soil density, moisture content, sieve analysis, etc.) required for an ideal Seed-Idriss Simplified Procedure. For boreholes having acceptable penetration tests, liquefaction analysis is performed using recorded density, moisture, and sieve test values or using averaged test values of similar materials.

The Seed-Idriss Simplified Procedure for liquefaction evaluation was developed primarily for clean sand and silty sand. As described above, results depend greatly on accurate evaluation of in-situ soil density as measured by the number of soil penetration blow counts using an SPT sampler. However, many of the Holocene alluvial deposits in the study area contain a significant amount of gravel. In the past, gravelly soils were considered not to be susceptible to liquefaction because the high permeability of these soils presumably would allow the dissipation of pore pressures before liquefaction could occur. However, liquefaction in gravelly soils has been observed during earthquakes, and recent laboratory studies have shown that gravelly soils are susceptible to liquefaction (Ishihara, 1985; Harder and Seed, 1986; Budiman and Mohammadi, 1995; Evans and Zhou, 1995; and Sy and others, 1995). SPT-derived density measurements in gravelly soils are unreliable and generally too high. They are likely to lead to overestimation of the density of the soil and, therefore, result in an underestimation of the liquefaction susceptibility. To identify potentially liquefiable units where the N values appear to have been affected by gravel content, correlations were made with boreholes in the same unit where the N values do not appear to have been affected by gravel content.

## LIQUEFACTION ZONES

### Criteria for Zoning

Areas underlain by materials susceptible to liquefaction during an earthquake were included in liquefaction zones using criteria developed by the Seismic Hazards Mapping Act Advisory Committee and adopted by the SMGB (DOC, 2000). Under those guideline criteria, liquefaction zones are areas meeting one or more of the following:

1. Areas known to have experienced liquefaction during historical earthquakes

2. All areas of uncompacted artificial fill containing liquefaction-susceptible material that are saturated, nearly saturated, or may be expected to become saturated

3. Areas where sufficient existing geotechnical data and analyses indicate that the soils are potentially liquefiable

4. Areas where existing geotechnical data are insufficient

In areas of limited or no geotechnical data, susceptibility zones may be identified by geologic criteria as follows:

a) Areas containing soil deposits of late Holocene age (current river channels and their historic floodplains, marshes and estuaries), where the M7.5-weighted peak acceleration that has a 10 percent probability of being exceeded in 50 years is greater than or equal to 0.10 g and the water table is less than 40 feet below the ground surface; or

b) Areas containing soil deposits of Holocene age (less than 11,000 years), where the M7.5-weighted peak acceleration that has a 10 percent probability of being exceeded in 50 years is greater than or equal to 0.20 g and the historical high water table is less than or equal to 30 feet below the ground surface; or

c) Areas containing soil deposits of latest Pleistocene age (11,000 to 15,000 years), where the M7.5-weighted peak acceleration that has a 10 percent probability of being exceeded in 50 years is greater than or equal to 0.30 g and the historical high water table is less than or equal to 20 feet below the ground surface.

Application of SMGB criteria to liquefaction zoning in the Niles Quadrangle is summarized below.

**Areas of Past Liquefaction**

Knudsen and others (2000) compiled data from Tinsley and others (1998) and Youd and Hoose (1978) for earthquakes in the San Francisco Bay region. Tinsley and others (1998) compiled observations of evidence for liquefaction for the 1989 Loma Prieta earthquake. Youd and Hoose (1978) compiled them for earlier earthquakes, including 1868 Hayward and 1906 San Francisco earthquakes. The Knudsen and others (2000) digital database differs from earlier compilation efforts in that the observations were located on a 1:24,000-scale base map versus the smaller- scale base maps used in the earlier publications. Sites were reevaluated and some single sites were broken into two or more where the greater base-map scale allowed.

In the Niles Quadrangle, no areas of documented historical liquefaction are known. Youd and Hoose (1979) cite information from the 1906 earthquake stating that neither the Sunol Aqueduct nor the Hetch Hetchy aqueduct (site 144) nor the railroad (site 164) appears to have suffered any harm (Plate 1.2). However, recent paleoseismic trench investigations by Lienkaemper and others (2002) have uncovered evidence for liquefaction during the 1868 M 6.9 Hayward earthquake and for at least one other earlier

event at Tyson's Lagoon (Tule Pond) which is located between two strands of the Hayward Fault near the BART station (Plate 1.1).

Other ground failures reported during the 1906 earthquake within the Niles Quadrangle include two landslides (sites 163 and 165) (Lawson, 1908; Coffman and vonHake, 1973). Also, an increase in water and decrease in soil stability within a Western Pacific Railway tunnel that was under construction (site 165 dashed line) was also noted (Youd and Hoose, 1979).

**Artificial Fills**

In the Niles Quadrangle, there are only two small areas mapped as artificial fill, one of which underlies a railroad in the northeast corner of the quadrangle and the other filling part of Tule's Pond. The engineering of the fill at Tule's Pond is unknown but this area is included within the zone of required investigation due to shallow ground water and because the fill overlies Holocene alluvial fan deposits. The fill underlying the railroad is thought to be properly engineered and is not included in the zone of required investigation as it overlies Holocene alluvial fan deposits that are not included in the zone.

**Areas with Sufficient Existing Geotechnical Data**

Borehole logs that include penetration test data and sufficiently detailed lithologic descriptions were used to quantitatively analyze liquefaction potential. These areas with sufficient geotechnical data were evaluated for zoning based on the liquefaction potential determined by the Seed-Idriss Simplified Procedure. In Holocene alluvial deposits that cover much of area west of the East Bay Hills, most of the borehole logs that were analyzed using the Seed-Idriss Simplified Procedure contain sediment layers that may liquefy under the expected earthquake loading. These areas containing saturated potentially liquefiable material with corresponding depths as shown in Table 1.3 are included in the liquefaction zone of required investigation.

Based on geologic interpretation of the thickness of Holocene alluvial fan deposits across the Alameda Creek alluvial fan and the presence of shallow ground water, most of the flatlands east of the Hayward Fault within the Niles Quadrangle are included within the liquefaction zone of required investigation. To the west of the Hayward Fault, where ground water is deeper, the eastern edge of the zone was defined where Pleistocene fan deposits are saturated but overlying Holocene deposits are not. Pleistocene fan deposits are interpreted to be less susceptible to liquefaction than Holocene deposits, being more dense and compacted (Tables 1.2 and 1.3). Areas where depth to the top of the Pleistocene deposits is less than the depth to the highest historical ground water (thus, Holocene deposits are not saturated) were not included in the zone of required investigation.

**Areas with Insufficient Existing Geotechnical Data**

Sufficient geotechnical data were not available for most upland valley areas, stream deposits along Niles canyon, in Sunol Valley and along Arroyo de la Laguna. In Sunol

Valley, despite having only a few geotechnical boreholes evaluated for liquefaction quantitatively, other geotechnical boreholes (Treadwell & Rollo, Inc., 2001) and field reconnaissance at one of the Mission Valley Rock quarries provided enough qualitative information for geologic interpretation of the sub-surface deposits. Based on geologic interpretation of thickness of Holocene deposits (generally less than 20 feet) and depth to ground water in Sunol Valley (20 to 30 feet), the areas mapped as Holocene stream terrace deposits (Qht) along Alameda Creek are not included in the zone of required of investigation. Modern stream and artificial channels (Qhc and ac) and latest Holocene stream terrace deposits (Qhty) along Alameda Creek in Sunol Valley are included in the zone of required investigation due to shallow ground water close to Alameda Creek.

All stream terrace deposits along Arroyo de la Laguna are included in the zone of required investigation due to the loose sandy deposits observed in the field. Also observed in the field were recent flood deposits about 10 feet below the mapped Holocene stream terrace deposits (Qht).

All modern stream channel deposits and Holocene stream terrace deposits along Niles Canyon are included in the zone of required investigation. Older stream terrace deposits (Qt, Qpt and Qot) are not included in the zone of required investigation, these probably being denser and unsaturated. Holocene alluvium (Qha) at the foot of Stoneybrook Canyon is included in the zone of required investigation because of the likely shallow ground water. Holocene alluvial fan deposits along Niles Canyon are included in the zone of required investigation if they are less than about 40 feet above the modern stream channel. Polygons that have been mapped as latest Pleistocene to Holocene and early to middle Pleistocene undifferentiated alluvial deposits (Qa and Qoa respectively) in upland valleys in the eastern half of the quadrangle, are not included in the zone of required investigation due to their age, limited extent and fine-grained nature as observed during field reconnaissance.

## ACKNOWLEDGMENTS

The authors would like to thank Kathleen Livermore with the city of Fremont, Norman Payne with the city of Hayward, Grant Cramond with the city of Union City, Ray Collier with the city of Newark and Gwen Ling with Caltrans. We thank all the staff in the building, engineering and planning departments who arranged access and provided assistance in retrieving geotechnical data from files maintained by the respective cities and the Caltrans archives in Sacramento. Thanks to the Regional Water Quality Control Board who provided ground-water data for Alameda County. Thanks go to Chris Hitchcock, William Lettis and Associates, who provided additional reports from monitoring wells collected from the Alameda County Water District, Tom O'Brien with Harlan Tait Assoicates for use of a geotechnical report describing gravels deposits in the Quarry Lakes regional Preserve in Fremont. Thanks go to Mort Calvert of Mission Valley Rock for allowing access to some of the gravel quarries in Sunol Valley and use of geotechnical reports describing the gravel deposits.

At CGS, special thanks to Al Barrows and Ralph Loyd for their technical reviews; Marvin Woods, Teri McGuire, Bob Moskovitz and Barbara Wanish for their GIS operations and database support; and Chanie Abuye for assistance with collection and input of geotechnical borehole data into the database. Thanks to Barbara Wanish who prepared the formal GIS liquefaction hazard zone maps for this report.

## REFERENCES

American Society for Testing and Materials, 1999, Standard test method for penetration test and split-barrel sampling of soils, Test Method D1586-99, *in* Annual Book of ASTM Standards, v. 4.08.

Atwater, B.F., Hedel, C.W. and Helley, E.J., 1977, Late Quaternary depositional history, Holocene sea-level changes, and vertical crustal movement, southern San Francisco Bay, California: U.S. Geological Survey Professional Paper 1014, 15 p.

Barlock, V.E., 1989, Sedimentology of the Livermore Gravels (Miocene-Pleistocene), southern Livermore Valley, California, US Geological Survey Open-File Report 89-131, 93 p.

Borcherdt, G., 1988, Soil Development and displacement along the Hayward Fault, California Division of Mines and Geology Open-File Report 88-12, 124 p.

Bryant, W.A., Martin, R., Wong, P., Maldonado, D., Wampole, J. and Dixon, D. 2001, GIS files of official Alquist-Priolo earthquake fault zones, northern and eastern region: California Department of Conservation, California Geological Survey, CGS CD 2001-06.

Budiman, J.S. and Mohammadi, J., 1995, Effect of large inclusions on liquefaction of sands, *in* Evans, M.D. and Fragaszy, R.J., *editors*, Static and Dynamic properties of Gravelly Soils: American Society of Civil Engineers Geotechnical Special Publication no. 56, p. 48-63.

Bull, W.B., 1991, Geomorphic responses to climatic change: Oxford University Press, New York, 326 p.

California Department of Conservation, Division of Mines and Geology, 1997, Guidelines for evaluating and mitigating seismic hazards in California: California Division of Mines and Geology Special Publication 117, 74 p.

California Department of Conservation, Division of Mines and Geology, 2000, Recommended criteria for delineating seismic hazard zones in California: California Division of Mines and Geology Special Publication 118, 12 p.

Clark, W.O., 1915, Ground-water Resources of the Niles cone and adjacent areas, California: US Geological Survey Water-Supply Paper 345-H, 168 p.

Coffman, J.L. and vonHake, C.A., 1973, Earthquake history of the United States (revised edition): U.S. Environmental Data Service, Publication 41-1, 208 p.

Collins, J., 2001, Historic drainage patterns of the Alameda watershed, presentation to the Alameda Creek flows Workshop #1, 11p.

Department of Water Resources, 1966, Evaluation of ground-water resources: Livermore and Sunol Valleys: Geology, Bulletin 118-2, Appendix A, 79 p.

Department of Water Resources, 1967, Evaluation of ground-water resources: South Bay: Geology, Bulletin 118-1, Appendix A, 153 p.

Department of Water Resources, 1968, Evalutation of ground-water resources: South Bay, Volume 1: Fremont Study Area, Bulletin 118-1, 117 p.

Department of Water Resources, 1974, Evaluation of ground water resources: Livermore and Sunol Valleys, Bulletin 118-2, 153 p.

Department of Water Resources, 1975, Ground water basin protection projects: Fremont salinity barrier, Bulletin 147-2, 48 p.

Evans, M.D. and Zhou, S., 1995, Liquefaction behaviour of sand-gravel composites: American Society of Civil Engineers, Journal of Geotechnical Engineering, v. 121, no. 3, p. 287-298.

Goldman, H.B., 1969, Geology of the San Francisco Bay, *in* Goldman, H. B., *editor*, Geologic and engineering aspects of the San Francisco Bay fill: California Division of Mines and Geology Special Report 97, p. 9-29.

Graymer, R.W., Jones, D.L. and Brabb, E.E., 1996, Preliminary geologic map emphasizing bedrock formations in Alameda County, California; A digital database: U.S. Geological Survey Open-File Report 96-252.

Harder, L.F. and Seed, H.B., 1986, Determination of penetration resistance for coarse-grained soils using the Becker hammer drill: University of California at Berkeley, College of Engineering, Earthquake Engineering Research Center, report no. UCB/EERC-86/06, 126 p.

Harlan Tait Associates, 1995, Appendices from Basic Design Report for the Rehabilitation for the Quarry Pits Rehabilitation Project, report submitted to Alameda County Water District.

Helley, E.J., LaJoie, K.R., Spangle, W.E. and Blair, M.L., 1979, Flatland deposits of the San Francisco Bay region, California—their geology and engineering properties, and their importance to comprehensive planning: U.S. Geological Survey Professional Paper 943, scale 1:125,000.

Helley, E.J. and Graymer, R.W., 1997, Quaternary geology of Alameda County, and parts of Contra Costa, Santa Clara, San Mateo, San Francisco, Stanislaus, and San Joaquin counties, California; a digital database: U.S. Geological Survey Open-File Report 97-97, 2 sheets.

Ishihara, K., 1985, Stability of natural deposits during earthquakes, *in* Proceedings of the Eleventh International Conference on Soil Mechanics and Foundation Engineering, San Francisco, v. 1, p. 321-376.

Kelson, K.I., Simpson, G.D., Haraden, C.C., and T.L. Sawyer, 1993, Late Quaternary surficial deformation of the Southern East Bay Hills, San Francisco Bay Region, California, Report to U.S. Geological Survey NEHRP, 29 p.

Knudsen, K.L., Sowers, J.M., Witter, R.C., Wentworth, C.M., Helley, E.J., Nicholson, R.S., Wright, H.M. and Brown, K.H., 2000, Preliminary maps of Quaternary deposits and liquefaction susceptibility, nine-county San Francisco Bay region, California; a digital database: U.S. Geological Survey Open-File Report 00-444.

Koltermann, C.E., 1994, Geologic modeling of spatial variability in sedimentary environments for ground-water flow simulation: Ph.D. dissertation, Stanford University, California.

Koltermann, C.E. and Gorelick, S.M., 1992, Paleoclimatic signature in terrestrial flood deposits: Science, v. 256, p. 1775-1782.

Lawson, A.C., chairman, 1908, The California earthquake of April 18, 1906; Report of the State Earthquake Investigation Commission: Carnegie Institute Washington Publication 87, v. 1, 451 p. (Reprinted, 1969).

Lienkaemper, J.J., 1992, Map of recently active traces of the Hayward Fault, Alameda and Contra Costa counties, California: U.S. Geological Survey Miscellaneous Field Studies Map MF-2196, scale 1:24,000.

Lienkaemper, J.L., Dawson, T.E., Personius, S.F., Seitz, G.G., Reidy, L.M. and D.P. Schwartz, 2002, A record of large earthquakes on the southern Hayward Fault for the past 500 years: Bulletin of the Seismological Society of America, v. 92, no. 7, p. 2637-2658.

Luhdorff and Scalmanini Consulting Engineers, 1993, Ground-water and aggregate resources, Sunol Valley, report prepared for the San Francisco Water Department, 31 p.

National Research Council, 1985, Liquefaction of soils during earthquakes: National Research Council Special Publication, Committee on Earthquake Engineering, National Academy Press, Washington, D.C., 240 p.

Petersen, M.D., Bryant, W.A., Cramer, C.H., Cao, T., Reichle, M.S., Frankel, A.D., Lienkaemper, J.J., McCrory, P.A. and Schwartz, D.P., 1996, Probabilistic seismic

hazard assessment for the State of California: California Department of Conservation, Division of Mines and Geology, Open-File Report 96-08; also U.S. Geological Survey Open-File Report 96-706, 33 p.

Radbruch, D.H., 1959, Former shoreline features along the east side of San Francisco Bay, California: U.S. Geological Survey Miscellaneous Geologic Investigations Map I-298, scale 1:48,000.

Rogers, J.D. and Figuers, S.H., 1992, Late Quaternary stratigraphy of the East Bay plain, *in* Borchardt, Glenn and others, *editors*, Proceedings of the Second Conference on earthquake hazards in the eastern San Francisco Bay Area: California Department of Conservation, Division of Mines and Geology Special Publication 113, p 19-28.

Seed, H.B. and Idriss, I.M., 1971, Simplified procedure for evaluating soil liquefaction potential: Journal of the Soil Mechanics and Foundations Division of ASCE, v. 97: SM9, p. 1,249-1,273.

Seed, H.B. and Idriss, I.M., 1982, Ground motions and soil liquefaction during earthquakes: Monograph Series, Earthquake Engineering Research Institute, Berkeley, California, 134 p.

Seed, H.B., Idriss, I.M. and Arango, I., 1983, Evaluation of liquefaction potential using field performance data: Journal of Geotechnical Engineering, v. 109, no. 3, p. 458-482.

Seed, H.B., Tokimatsu, K., Harder, L.F., and Chung, R.M., 1985, Influence of SPT procedures in soil liquefaction resistance evaluations: Journal of Geotechnical Engineering, ASCE, v. 111, no. 12, p. 1,425-1,445.

Seed, R.B. and Harder, L.F., 1990, SPT-based analysis of cyclic pore pressure generation and undrained residual strength: Proceedings of the H. Bolton Seed Memorial Symposium, v. 2, p. 351-376.

Sloan, D., 1992, The Yerba Buena mud: record of the last interglacial predecessor of the San Francisco Bay, California: Geological Society of America Bulletin, v. 104, p. 716-727.

Sloan, D. and Aubrey, B., 1991, Pleistocene sea level history of the San Francisco Bay, Abstracts with Programs, Cordilleran Section Meeting: Geological Society of America, San Francisco, v. 23, p. 98.

Smith, T.C., 1996, Preliminary maps of seismic hazard zones and draft guidelines for evaluating and mitigating seismic hazards: California Geology, v. 49, no. 6, p. 147-150.

Southern California Earthquake Center, 1999, Recommended procedures for implementation of DMG Special Publication 117 guidelines for analyzing and

mitigating liquefaction in California: Southern California Earthquake Center, University of Southern California, 63 p.

Sowers, J.M., unpublished mapping, to be incorporated in revision to Knudsen, K.L., Sowers, J.M., Witter, R.C., Wentworth, C.M., Helley, E.J., Nicholson, R.S., Wright, H.M., and Brown, K.H., 2000, Preliminary maps of Quaternary deposits and liquefaction susceptibility, nine-county San Francisco Bay region, California: a digital database, U.S. Geological Survey, Open-File Report 00-444, scale 1:24,000.

Sy, A., Campanella, R.G. and Stewart, R.A., 1995, BPT-SPT correlations for evaluations of liquefaction resistance in gravelly soils, *in* Evans, M.D. and Fragaszy, R.J., *editors*, Static and Dynamic Properties of Gravelly Soils: American Society of Civil Engineers Geotechnical Special Publication no. 56, p. 1-19.

Tinsley, J.C., Youd, T.L., Perkins, D.M. and Chen, A.T.F., 1985, Evaluating liquefaction potential, *in* Ziony, J.I., *editor*, Evaluating earthquake hazards in the Los Angeles region — An earth science perspective: U.S. Geological Survey Professional Paper 1360, p. 263-316.

Tinsley, J.C., III, Egan, J.A., Kayen, R.E., Bennett, M.J., Kropp, A. and Holzer, T.L., 1998, Appendix: maps and descriptions of liquefaction and associated effects, *in* Holzer, T.L, *editor*, The Loma Prieta, California, earthquake of October 17, 1989: liquefaction, strong ground motion and ground failure: U.S. Geological Survey Professional Paper 1551-B, p. B287-314, scale 1:100,000.

Trask, P.D. and Rolston, J.W., 1951, Engineering geology of San Francisco Bay, California: Geological Society of America Bulletin, v. 62, p. 1079-1110.

Treadwell & Rollo, Inc., 2001, Resource investigation, Mission Valley Rock Quarry, Sunol, California, 12 p. plus appendices.

Youd, T.L., 1973, Liquefaction, flow and associated ground failure: U.S. Geological Survey Circular 688, 12 p.

Youd, T.L., 1991, Mapping of earthquake-induced liquefaction for seismic zonation: Earthquake Engineering Research Institute, Proceedings, Fourth International Conference on Seismic Zonation, v. 1, p. 111-138.

Youd, T.L. and Perkins, D.M., 1978, Mapping liquefaction-induced ground failure potential: Journal of Geotechnical Engineering, v. 104, p. 433-446.

Youd, T.L. and Hoose, S.N., 1978, Historic ground failures in orthern California triggered by earthquakes: U.S. Geological Survey Professional Paper 993, scales 1:250,000 and 1:24,000.

Youd, T.L. and Idriss, I.M., 1997, *editors*, Proceedings of the NCEER workshop on evaluation of liquefaction resistance of soils: National Center for Earthquake Engineering Research Technical Report NCEER-97-0022, 276 p.

Youd, T.L., Idriss, I.M., Andrus, R.D., Arango, I., Castro, G., Christian, J.T., Dobry, R., Finn, W.D.L., Harder, L.F. Jr., Hynes, M.E., Ishihara, K., Koester, J.P., Liao, S.S.C., Marcusson, W.F., Martin, G.R., Mitchell, J.K., Moriwaki, Y., Power, M.S., Robertson, P.K., Seed, R.B. and Stokoe, K.H., 2001, Liquefaction resistance of soils; Summary report from the 1996 NCEER/NSF workshops on evaluation of liquefaction resistance of soils: Journal of Geotechnical and Geoenvironmental Engineering, October 2001, p. 817-833.

# SECTION 2
# EARTHQUAKE-INDUCED LANDSLIDE EVALUATION REPORT

## Earthquake-Induced Landslide Zones in the Niles 7.5-Minute Quadrangle, Alameda County, California

**By**
**Mark O. Wiegers**

**California Department of Conservation**
**California Geological Survey**

### PURPOSE

The Seismic Hazards Mapping Act (the Act) of 1990 (Public Resources Code, Chapter 7.8, Division 2) directs the California Department of Conservation (DOC), Division of Mines and Geology (DMG) [now called California Geological Survey (CGS)] to delineate Seismic Hazard Zones. The purpose of the Act is to reduce the threat to public health and safety and to minimize the loss of life and property by identifying and mitigating seismic hazards. Cities, counties, and state agencies are directed to use seismic hazard zone maps prepared by CGS in their land-use planning and permitting processes. The Act requires that site-specific geotechnical investigations be performed prior to permitting most urban development projects within the hazard zones. Evaluation and mitigation of seismic hazards are to be conducted under guidelines established by the California State Mining and Geology Board (DOC, 1997a). The text of this report is on the Internet at http://gmw.consrv.ca.gov/shmp/SHMPsp117.asp

Following the release of DMG Special Publication 117 (DOC, 1997a), agencies in the Los Angeles metropolitan region sought more definitive guidance in the review of geotechnical investigations addressing landslide hazards. The agencies made their request through the Geotechnical Engineering Group of the Los Angeles Section of the American Society of Civil Engineers (ASCE). This group convened an implementation committee in 1998 under the auspices of the Southern California Earthquake Center (SCEC). The committee, which consisted of practicing geotechnical engineers and engineering geologists, released an overview of the practice of landslide analysis, evaluation, and mitigation techniques (SCEC, 2002). This text is also on the Internet at: http://www.scec.org/

This section of the evaluation report summarizes seismic hazard zone mapping for earthquake-induced landslides in the Niles 7.5-Minute Quadrangle. Section 1 (addressing liquefaction) and Section 3 (addressing earthquake shaking) complete the report, which is one of a series that summarizes the preparation of seismic hazard zone maps within the state (Smith, 1996). Additional information on seismic hazard zone mapping in California can be accessed on the California Geological Survey's Internet page: http://www.consrv.ca.gov/CGS/index.htm

## BACKGROUND

Landslides triggered by earthquakes historically have been a significant cause of earthquake damage. In California, large earthquakes such as the 1971 San Fernando, 1989 Loma Prieta, and 1994 Northridge earthquakes triggered landslides that were responsible for destroying or damaging numerous structures, blocking major transportation corridors, and damaging life-line infrastructure. Areas that are most susceptible to earthquake-induced landslides are steep slopes in poorly cemented or highly fractured rocks, areas underlain by loose, weak soils, and areas on or adjacent to existing landslide deposits. These geologic and terrain conditions exist in many parts of California, including numerous hillside areas that have already been developed or are likely to be developed in the future. The opportunity for strong earthquake ground shaking is high in many parts of California because of the presence of numerous active faults. The combination of these factors constitutes a significant seismic hazard throughout much of California, including the hillside areas of the Niles Quadrangle.

## METHODS SUMMARY

The mapping of earthquake-induced landslide hazard zones presented in this report is based on the best available terrain, geologic, geotechnical, and seismological data. If unavailable or significantly outdated, new forms of these data were compiled or generated specifically for this project. The following were collected or generated for this evaluation:

- Digital terrain data were used to provide an up-to-date representation of slope gradient and slope aspect in the study area.

- Geologic mapping was used to provide an accurate representation of the spatial distribution of geologic materials in the study area. In addition, a map of existing landslides, whether triggered by earthquakes or not, was prepared.

- Geotechnical laboratory test data were collected and statistically analyzed to quantitatively characterize the strength properties and dynamic slope stability of geologic materials in the study area.

- Seismological data in the form of CGS probabilistic shaking maps and catalogs of strong-motion records were used to characterize future earthquake shaking within the mapped area.

The data collected for this evaluation were processed into a series of GIS layers using commercially available software. A slope stability analysis was performed using the Newmark method of analysis (Newmark, 1965), resulting in a map of landslide hazard potential. The earthquake-induced landslide hazard zone was derived from the landslide hazard potential map according to criteria developed in a CGS pilot study (McCrink and Real, 1996; McCrink, 2001) and adopted by the State Mining and Geology Board (DOC, 2000).

## SCOPE AND LIMITATIONS

The methodology used to make this map is based on earthquake ground-shaking estimates, geologic material-strength characteristics and slope gradient. These data are gathered from a variety of outside sources. Although the selection of data used in this evaluation was rigorous, the quality of the data is variable. The State of California and the Department of Conservation make no representations or warranties regarding the accuracy of the data gathered from outside sources.

Earthquake-induced landslide zone maps are intended to prompt more detailed, site-specific geotechnical investigations as required by the Act. As such, these zone maps identify areas where the potential for earthquake-induced landslides is relatively high. Due to limitations in methodology, it should be noted that these zone maps do not necessarily capture all potential earthquake-induced landslide hazards. Earthquake-induced ground failures that are not addressed by this map include those associated with ridge-top spreading and shattered ridges. It should also be noted that no attempt has been made to map potential run-out areas of triggered landslides. It is possible that such run-out areas may extend beyond the zone boundaries. The potential for ground failure resulting from liquefaction-induced lateral spreading of alluvial materials, considered by some to be a form of landsliding, is not specifically addressed by the earthquake-induced landslide zone or this report. See Section 1, Liquefaction Evaluation Report for the Niles Quadrangle, for more information on the delineation of liquefaction zones.

The remainder of this report describes in more detail the mapping data and processes used to prepare the earthquake-induced landslide zone map for the Niles Quadrangle. The information is presented in two parts. Part I covers physiographic, geologic and

engineering geologic conditions in the study area. Part II covers the preparation of landslide hazard potential and landslide zone maps.

# PART I

# PHYSIOGRAPHY

## Study Area Location and Physiography

The Niles 7.5-Minute Quadrangle map lies within Alameda County and covers approximately 60 square miles on the eastern side of San Francisco Bay. The map area includes a large part of the city of Fremont, smaller parts of the city of Newark and the Union City, a very small part of the city of Pleasanton and unincorporated portions of Alameda County.

The topography of the Niles Quadrangle ranges from flatlands to steep hillsides. About one third of the map area on the southwestern side consists of the nearly flat-lying East Bay Plain that borders San Francisco Bay. The western side of Sunol Valley is also a nearly flat area that extends into the eastern side of the map area. Relatively steep slopes of the East Bay Hills and the Diablo Range occupy the remainder of the quadrangle. Major ridges and peaks include Walpert Ridge, Sunol Ridge and Pleasanton Ridge in the northern part of the map area, and Mission Peak on the southeast. Elevations in the quadrangle range from 2,517 feet above sea level at the top of Mission Peak to less than 10 feet above sea level on the East Bay Plain in the southwestern corner.

The most prominent stream in the map area is Alameda Creek, which flows west through Niles Canyon. Niles Canyon is a deep, winding chasm through the crest of the East Bay Hills that carries drainage from the Livermore Valley, Sunol Valley and a portion of the Diablo Range south of Sunol Valley. Large gravel quarries have been excavated along Alameda Creek in the flatlands just west of the mouth of Niles Canyon. The gravel quarries are now managed as ground-water recharge basins. Palomares Creek and Sinbad Creek are two prominent tributaries of Alameda Creek that flow through deep canyons on the northern side of Niles Canyon. Several smaller streams south of Niles Canyon drain the western edge of the Diablo Range and flow onto the flatlands of the East Bay Plain, including Morrison Creek, Mission Creek and Agua Caliente Creek. On the flatlands, these streams have generally been diverted through developed areas in culverts or artificial channels.

Major developed areas in the Niles Quadrangle are concentrated on the East Bay Plain in the southwestern part of the map area and on the lower slopes of the Diablo Range. Many new homes have recently been constructed on gentle to moderately steep terrain in the Mission San Jose and Warm Springs regions of Fremont. The map area also includes the site of Mission San Jose, established by Spanish missionaries more than 200 years ago. Major highways include Interstate 880 in the southwestern part of the quadrangle, Interstate 680, which extends through the hills between Fremont and Sunol, and State

Route 84, which extends through Niles Canyon. A Union Pacific Railroad line also follows Niles Canyon.

### Digital Terrain Data

The calculation of slope gradient is an essential part of the evaluation of slope stability under earthquake conditions. An accurate slope gradient calculation begins with an up-to-date map representation of the earth's surface in the form of a digital topographic map. Within the Niles Quadrangle, two sources of terrain data were used: 1) digital contours derived from an airborne LIDAR (Light Detection and Ranging) system flown in May 2002 for areas within the city of Fremont; and 2) a U.S. Geological Survey digital elevation model (DEM) for areas outside of the Fremont digital terrain data.

Terrain data were provided by the city of Fremont in the form of digital two-foot contours. The contour data were converted to a DEM format with a 10-meter horizontal resolution and applied as a replacement of the USGS DEM data wherever available. It includes both natural slopes and slopes modified by mass grading for large developments. The vertical accuracy of this DEM is estimated to be on the order of one to two meters. Plate 2.1 shows the area where the Fremont terrain data are used.

The USGS DEM was prepared from the 7.5-minute quadrangle topographic contours generated from 1948 aerial photographs by photogrammetric methods and from plane table surveys. It is a Level 2 DEM that has a 10-meter horizontal resolution and a 7.5-meter vertical accuracy.

A slope map was made from the updated DEM using a third-order, finite difference, center-weighted algorithm (Horn, 1981). The DEM also was used to make a slope aspect map. The manner in which the slope and aspect maps were used to prepare the zone map will be described in subsequent sections of this report.

## GEOLOGY

### Bedrock and Surficial Geology

The primary source of bedrock geologic information used in this slope stability evaluation was the "Preliminary geologic map emphasizing bedrock formations in Alameda County, California: A digital database" by Graymer and others (1996). This digital geologic database was compiled at a resolution of 1:24,000 from previously published reports and from new mapping and field checking by Graymer and others (1996). The geology and structure of the southeast San Francisco Bay area is summarized in Graymer (1995). Geologic mapping by Dibblee (1980) was also reviewed. Quaternary surficial geologic mapping was prepared by J.M. Sowers (unpublished) at a scale of 1:24,000.

Geologists at the California Geological Survey merged the surficial and bedrock geologic maps, and contacts between surficial and bedrock units were modified in some areas to resolve differences between the two maps. Geologic field reconnaissance was performed

to assist in adjusting contacts and to review the lithology and structure of the various geologic units.

Bedrock in the Niles Quadrangle is characterized by two highly deformed Mesozoic basement assemblages that are unconformably overlain by Tertiary sedimentary rocks, minor Tertiary volcanic rocks and Quaternary sediments. These two Mesozoic basement complexes are the Franciscan Complex and the Great Valley Complex (Graymer, 2000).

The Franciscan Complex (geologic map symbol "fm") presumably underlies the entire study area at depth (Graymer and others, 1996) but is only exposed in one small fault-bound sliver along the Calaveras Fault at the eastern edge of the map area. This exposure is mapped as Franciscan Melange of Late Jurassic to Late Cretaceous age, which consists of crushed argillite with blocks of graywacke, basalt, chert and metamorphic rocks.

The Franciscan Complex is overlain by younger rocks elsewhere in the Niles Quadrangle. In the hills between the Calaveras Fault and Hayward Fault, the Franciscan Complex is structurally overlain by the Great Valley Complex along the Coast Range Thrust, a regionally extensive fault system that was formed by late Mesozoic subduction. In the flatland areas west of the Hayward Fault, the Franciscan Complex is directly overlain by thick Quaternary deposits with no intervening Cretaceous or Tertiary strata, apparently indicating that this area was once a topographic high and that intervening strata were either eroded away or never deposited. The Franciscan Complex is exposed in the Coyote Hills a few miles west of the map area.

The Great Valley Complex includes the Coast Range Ophiolite, which is composed of serpentinite, gabbro, diabase, basalt and keratophyre (altered silicic volcanic rock), and the Great Valley Sequence, which is composed of sandstone, conglomerate and shale of Jurassic and Cretaceous age (Graymer, 2000). The ophiolite rocks are the remnants of arc-related oceanic crust. The Great Valley Sequence consists of turbidites that were deposited on top of the crustal rocks. Ophiolitic rocks of the Great Valley Complex are not exposed in the map area; however, several units of the overlying Great Valley Sequence are extensively exposed, notably in Niles Canyon and on major ridges north of Niles Canyon. The Knoxville Formation (KJk) consists of silt and clay shale with thin interbeds of sandstone. The lower part contains thick pebble to cobble conglomerate beds (KJkc). The Oakland Conglomerate (Ko) consists of medium- to coarse-grained sandstone with prominent lenses of pebble to cobble conglomerate. An unnamed unit of sandstone, conglomerate and shale that is widely exposed in the Castro Valley area (Kcv) extends into a small area in the northern part of the map area. The base and top of this unit are bounded by faults (Graymer, 2000). The Redwood Canyon Formation (Kr) consists of fine- to coarse-grained sandstone with thin interbeds of mica-rich siltstone. The Pinehust Shale (Kp) consists of siliceous shale with interbedded sandstone and siltstone. Unnamed Cretaceous sedimentary rocks (KuII) consisting of graywacke, siltstone and mudstone underlie Sunol Ridge and Pleasanton Ridge in the northeastern part of the map area. These unnamed rocks contain lenses of pebble to boulder conglomerate (Kc) that are mapped locally. A second sequence of unnamed Cretaceous rocks (Ks) that consists of sandstone with siltstone and shale is also exposed in steep portions of the East Bay Hills both north and south of Niles Canyon.

Tertiary rocks in the map area include Paleocene to Miocene marine sedimentary rocks that unconformably overlie the Mesozoic basement rocks. One of these Tertiary marine units, the Briones Sandstone (Tbr) is a resistant ridge-forming unit that underlies some of the more prominent peaks and ridges in the map area, including the crest of Mission Peak. The Claremont Shale is also relatively extensive in the study area. Other Tertiary marine units are relatively limited in extent.

Tertiary marine rocks include the following units. Unnamed Paleocene rocks (Tpsu) primarily consist of siltstone, claystone and shale with some coarse glauconitic sandstone at the base. The Tolman Formation of Eocene (?) age includes medium- to coarse-grained glauconitic sandstone (Tts) and gray algal limestone interbedded with calcium-carbonate cemented sandstone and conglomerate (Ttls). An unnamed early Miocene unit (Tsh) exposed in Niles Canyon contains shale, sandstone, chert and dolomite with some dolomite-cemented conglomerate. The Sobrante Sandstone (Ts) consists of white, fine- to medium-grained sandstone. The Claremont Shale (Tcs) consists to brown siliceous shale with minor interbedded chert. This unit also contains light gray quartz sandstone and siltstone that locally is mapped separately (TccsI). The Oursan Sandstone (To) consists of greenish-gray sandstone with carbonate concretions. The Tice Shale (Tt) consists of brown siliceous shale.

Miocene to Plio-Pleistocene non-marine sedimentary rocks and minor volcanic rocks unconformably overlie the Tertiary marine rocks described above. The following Miocene non-marine units are mapped. The late Miocene Orinda Formation (Tor) consists of pebble to boulder conglomerate, conglomeratic sandstone and coarse- to medium-grained sandstone. Locally, the unit contains interlayered plagioclase porphyry diorite (Torv). Unnamed volcanic rocks (Tv) consisting of rhyolite, dacite and andesite tuff, breccia and volcanoclastic conglomerate with some basalt overlies the Orinda Formation in the northwestern part of the map area. The Livermore Gravels (QTl) of Pliocene and Pleistocene age consisting of poorly to moderately consolidated conglomerate, pebble- and cobble-bearing sand and coarse sand are exposed in the Sunol area. The Irvington Gravels (QTi) of Pliocene (?) and Pleistocene age are very similar to the Livermore Gravels exposed the Sunol area and consist of well-rounded pebbles and cobbles, pebble-bearing sand and coarse, cross-bedded sand. The Irvington Gravels have yielded abundant vertebrate fossils from the Pleistocene.

Unconsolidated Quaternary deposits overlie the bedrock units on the East Bay Plain, in Sunol Valley and in smaller alluvial areas and terraces in the hillside areas. Quaternary deposits in the map area are described in detail in Section 1.

**Structural Geology**

The study area is in a regime of transpressive deformation. Large-scale geologic structures in the study area include two major strike-slip faults and a number of reverse faults and folds.

The two major strike-slip faults in the study area are the Hayward Fault, which extends through the western and southern parts of the map area, and the Calaveras Fault, which

extends through the northeastern side of the map area. Both of these faults have been classified as active faults and are included in official fault-rupture hazard zones under the Alquist-Priolo Earthquake Fault Zone Act (DOC, 1997b). An active fault is defined as a fault that has had surface displacement during Holocene time.

The Hayward Fault is an active right-lateral strike-slip fault with an estimated slip rate of about 9mm per year. The Hayward Fault is actively creeping in the Niles and Hayward quadrangles, offsetting curbs, streets, buildings and other structures in numerous locations (Galehouse, 1992; Lienkaemper and Borchardt, 1992). The inferred active trace of the Hayward Fault has been mapped in detail by Lienkaemper (1992). Various other traces are shown on earlier geologic maps (Radbruch-Hall, 1974; Smith, 1980; Dibblee, 1980). South of the Niles Quadrangle, the Hayward Fault loses much of its geomorphic expression and dies out among a system of transpressive faults that extend along the eastern side of the Santa Clara Valley.

The Calaveras Fault is largely obscured by landslides in the Niles Quadrangle, but is well defined and exhibits Holocene displacement south of the map area. It loses much of its geomorphic expression and measurable seismicity north of the map area and dies out on the western side of the San Ramon Valley.

Other significant faults in the study area include the Mission Fault and the Warm Springs Fault. Neither of these faults is included in an Alquist-Priolo Earthquake Fault Zone for Special Studies. These faults, as well as several other faults that juxtapose Cretaceous and Tertiary units in the East Bay Hills, appear to have a compressional component of slip. The Mission Fault extends across the southwestern side of Mission Peak and juxtaposes non-marine rocks of the Orinda Formation against marine rocks of the Briones Sandstone. Based on several decades of micoseismicity data, it has been postulated that the Mission Fault accommodates a step-over of slip from the Calaveras Fault to the Hayward Fault (Andrews and others, 1992; Wong and Hemphill-Haley, 1992). The Warm Springs Fault is mapped south of Mission San Jose extending south into the Milpitas Quadrangle. A thermal spring and travertine deposits in the Warm Springs area in the southernmost part of the map area are likely associated with this fault. The fault appears to displace the Irvington Gravels, suggesting Quaternary displacement.

Bedding in Cretaceous and Tertiary units in the map area is generally steep and locally overturned, attesting to the considerable tectonic deformation that has taken place. Several northwest-southeast trending synclines have been mapped in the hills between the Hayward Fault and the Calaveras Fault (Graymer and others, 1996).

**Landslide Inventory**

As a part of the geologic data compilation, an inventory of existing landslides in the Niles Quadrangle was prepared by field reconnaissance, analysis of stereo-paired aerial photographs and a review of previously published landslide mapping (Geolith Consultants, 2000; Nilsen, 1975; Dibblee, 1980). Landslides were mapped at a scale of 1:24,000. For each landslide included on the map a number of characteristics (attributes) were compiled. These characteristics include the confidence of interpretation (definite,

probable and questionable) and other properties, such as activity, thickness, and associated geologic unit(s). Landslides rated as definite and probable were carried into the landslide zoning. Landslides rated as questionable were not carried into the landslide zoning due to the uncertainty of their existence. The completed landslide map was scanned, digitized, and the attributes were compiled in a database.

The map area includes a very large and striking landslide complex that encompasses virtually the entire southwestern slope of Mission Peak and its adjoining ridge to the northwest. This landslide complex consists of a steep, prominent headwall below the ridge and a series of large, deep-seated landslide blocks extending laterally downslope as much as 4,000 feet below the headwall. The landslide blocks are characterized by benched topography with local closed depressions. These landslide blocks host many smaller dormant and active landslides, including rock slides, earthflows and debris flows. The headwall area is a source of rockfalls and debris slides. Most of the landslide complex lies within parklands administered by the East Bay Regional Park District that will not likely be developed in the future. Below the parklands there are many new homes downslope from some of the landslides and, in some cases, on the lower parts of some probable deep landslide masses.

In 1998, a portion of the Mission Peak landslide complex failed spectacularly after a period of prolonged heavy rainfall during an abnormally wet rainy season generated by El Nino climatic conditions. The 1998 failure, visible for many miles around, involved relatively deep block sliding in the upper part of the failure and thick earthflow movement in the lower reaches. Significant rockfalls took place in the headscarp area over a period of several months after the initial failure. The 1998 failure is nearly one-mile long and 800 to 1400 feet wide in the middle regions. A detailed geologic/geotechnical investigation was performed to evaluate hazards from the Mission Peak landslide complex after the 1998 failure (Geolith Consultants, 2000). A detailed landslide map of the Mission Peak landslide was prepared by Geolith (2000). Some of that mapping was incorporated and modified for the landslide inventory prepared by CGS.

Another very large, deep-seated landslide complex is in the northeast part of the map area. This landslide complex encompasses virtually the entire northeastern side of Pleasanton Ridge and extends as much as two miles farther to the northwest into the Dublin Quadrangle, encompassing a well-known landslide called the Castlewood Country Club landslide. The landslide debris may be as much as several hundred feet deep. It is likely that the landslide originated in the Pleistocene (Rogers and Halliday, 1992).

Other landslide locations include steep slopes at the western end of Niles Canyon and along some of the steep tributary valleys north of Niles Canyon. Landslides are relatively sparse in the central part of the quadrangle between Interstate 680 and Niles Canyon. The areal distribution of landslides identified in the map area is shown on Plate 1.2.

# ENGINEERING GEOLOGY

## Geologic Material Strength

To evaluate the stability of geologic materials under earthquake conditions, the geologic map units described above were ranked and grouped on the basis of their shear strength. Generally, the primary source for shear-strength measurements is geotechnical reports prepared by consultants on file with local government permitting departments. Shear-strength data for the units identified on the Niles Quadrangle geologic map were obtained from the community development departments of the city of Fremont and Alameda County (see Appendix A). The locations of rock and soil samples taken for shear testing within the Niles Quadrangle are shown on Plate 2.1. Shear tests from the adjoining Hayward, Newark and Milpitas quadrangles were used to augment data for several geologic formations for which little or no shear test information was available within the Niles Quadrangle.

Shear strength data gathered from the above sources were compiled for each geologic map unit. Geologic units were grouped on the basis of average angle of internal friction (average phi) and lithologic character. Average (mean or median) phi values for each geologic map unit and corresponding strength group are summarized in Table 2.1. For most of the geologic strength groups in the map area, a single shear strength value was assigned and used in our slope stability analysis. A geologic material strength map was made based on the groupings presented in Table 2.1 and Table 2.2. This map provides a spatial representation of material strength for use in the slope stability analysis.

Several formations were subdivided further to account for potentially greater instability on slopes with adverse bedding conditions, as discussed in the following section. Formations that were subdivided further include Kcv, Ko, Kr, Kc, KJkc, KsVII, KuII, Tor, Tr, Tt, Tsso, Tssc, Tc and To.

## Adverse Bedding Conditions

Adverse bedding conditions are an important consideration in slope stability analyses. Adverse bedding conditions occur where the dip direction of bedded sedimentary rocks is roughly the same as the slope aspect, and where the dip magnitude is less than the slope gradient. Under these conditions, landslides can slip along bedding surfaces due to a lack of lateral support.

To account for adverse bedding in our slope stability evaluation, we used geologic structural data in combination with digital terrain data to identify areas with potentially adverse bedding, using methods similar to those of Brabb (1983). The structural data, derived from the geologic map database, were used to categorize areas of common bedding dip direction and magnitude. The dip direction was then compared to the slope aspect and, if the same, the dip magnitude and slope gradient categories were compared. If the dip magnitude category was less than or equal to the slope gradient category, but greater than 25 percent (4:1 slope), the area was marked as a potential adverse bedding area.

The geologic units Kcv, Ko, Kr, Kc, KJkc, KsVII, KuII, Tor, Tr, Tt, Tsso, Tssc, Tc and To were subdivided based on shear strength differences between coarse-grained (higher strength) and fine-grained (lower strength) lithologies. Shear strength values for the fine- and coarse-grained lithologies were then applied to areas of favorable and adverse bedding orientation, which were determined from structural and terrain data as discussed above. It was assumed that coarse-grained material strength dominates where bedding dips into a slope (favorable bedding) while fine-grained material strength dominates where bedding dips out of a slope (adverse bedding). The geologic material strength map was modified by assigning the lower, fine-grained shear strength values to areas where potential adverse bedding conditions were identified. The favorable and adverse bedding shear strength parameters for the geologic units Kcv, Ko, Kr, Kc, KJkc, KsVII, KuII, Tor, Tr, Tt, Tsso, Tssc, Tc and To are included in Table 2.1.

As discussed latter in this report, a dip slope analysis was performed in the map area to identify areas of potentially adverse bedding. Adverse bedding conditions occur where the dip direction of bedded sedimentary rocks is roughly the same as the slope aspect, and where the dip magnitude is less than the slope gradient. Most beds in the map area dip steeper (> 45 degrees) than the topographic slopes. As a result, very few areas of potentially adverse bedding were identified in the map area.

**Existing Landslides**

As discussed later in this report, the criteria for landslide zone mapping state that all existing landslides that are mapped as definite or probable are automatically included in the landslide zone of required investigation. Therefore, an evaluation of shear strength parameters for existing landslides is not necessary for the preparation of the zone map. However, in the interest of completeness for the material strength map, to provide relevant material strength information to project plan reviewers, and to allow for future revisions of our zone mapping procedures, we have collected and compiled shear strength data considered representative of existing landslides within the quadrangle.

The strength characteristics of existing landslides (Qls) must be based on tests of the materials along the landslide slip surface. Ideally, shear tests of slip surfaces formed in each mapped geologic unit would be used. However, this amount of information is rarely available, and for the preparation of the earthquake-induced landslide zone map it has been assumed that all landslides within the quadrangle have the same slip surface strength parameters. We collect and use primarily “residual” strength parameters from laboratory tests of slip surface materials tested in direct shear or ring shear test equipment. Back-calculated strength parameters, if the calculations appear to have been performed appropriately, also have been used. For the Niles Quadrangle, a residual direct shear test from the Penetencia Creek landslide located east of San Jose was used as a characteristic residual strength value for landslides. This test was performed on a well-developed landslide slip surface that was obtained from a deep borehole in the landslide mass. This test yielded an internal friction of angle (phi value) of 12 degrees.

**NILES QUADRANGLE**
**SHEAR STRENGTH GROUPS**

| | Formation Name | Number Tests | Mean/Median Phi (deg) | Mean/Median Group Phi (deg) | Mean/Median Group C (psf) | No Data: Similar Lithology | Phi Values Used in Stability Analyses |
|---|---|---|---|---|---|---|---|
| GROUP 1 | KJk* | 11 | 32/32 | 30/32 | 748/620 | Kc(fbc) | 32 |
| | Kcv(fbc)* | 15 | 33/33 | | | KsVII(fbc) | |
| | Ko(fbc)* | 9 | 34/35 | | | KJkc(fbc) | |
| | Kr(fbc)* | 3 | 28/33 | | | To(fbc) | |
| | Tbr** | 9 | 29/32 | | | Tsso(fbc) | |
| | | | | | | Tssc(fbo) | |
| GROUP 2 | Kcv(abc)* | 22 | 27/26 | 28/27 | 585/500 | Kc(fbc) | 28 |
| | Kull(fbc)* | 11 | 31/27 | | | Kp | |
| | Tcs* | 4 | 26/30 | | | TccsI | |
| | af | 31 | 27/29 | | | To(abc) | |
| | | | | | | Tord | |
| | | | | | | Tpsu | |
| | | | | | | Tr(fbc) | |
| | | | | | | Tshs | |
| | | | | | | Tsso(abc) | |
| | | | | | | Tssc(abc) | |
| | | | | | | Tt(fbc) | |
| | | | | | | Ttls | |
| GROUP 3 | fm* | 9 | 21/18 | 23/23 | 748/660 | QTl | 23 |
| | KJkc(abc)* | 3 | 22/25 | | | KsVII(abc) | |
| | Ko(abc)* | 11 | 23/24 | | | Tr(abc) | |
| | QTi** | 76 | 23/21 | | | Tt(abc) | |
| | Qa** | 67 | 23/23 | | | ac | |
| | Tor(fbc) | 3 | 26/24 | | | | |
| GROUP 4 | Kr(abc)* | 12 | 17/13 | 17/16 | 842/600 | | 17 |
| | Kull(abc)* | 7 | 17/16 | | | | |
| | Tor(abc) | 14 | 14/16 | | | | |
| | Qhbm*** | 10 | 17/20 | | | | |
| GROUP 5 | Qls | 1 | 12 | 12 | 745 | | 12 |

abc = adverse bedding condition, fine-grained material strength
fbc = favorable bedding condition, coarse-grained material strength
* includes tests from Hayward Quadrangle
** includes tests from Milpitas Quadrangle
*** includes tests from Newark Qudrangle

Formation name abbreviations from USGS Open File 96-252 (Graymer and others, 1996)

**Table 2.1. Summary of the Shear Strength Statistics for the Niles Quadrangle.**

| SHEAR STRENGTH GROUPS FOR THE NILES 7.5-MINUTE QUADRANGLE | | | | |
|---|---|---|---|---|
| GROUP 1 | GROUP 2 | GROUP 3 | GROUP 4 | GROUP 5 |
| | | | | |
| KJk | Kcv(abc) | fm | Kr(abc) | Qls |
| Kcv(fbc) | KuII(fbc) | KJkc(abc) | Kull(abc) | |
| Ko(fbc) | Kc(abc) | KsVII(abc) | Tor(abc) | |
| Kr(fbc) | Kp | Ko(abc) | Qhbm | |
| KJkc(fbc) | Tcs | Tr(abc) | | |
| Kc(fbc) | TccsI | Tt(abc) | | |
| KsVII(fbc) | To(abc) | Tor(fbc) | | |
| Tbr | Tr(fbc) | QTi | | |
| Tsso(fbc) | Tt(fbc) | QTl | | |
| Tssc(fbc) | Tshs | Qa | | |
| To(fbc) | Tsso(abc) | ac | | |
| | Tssc(abc) | | | |
| | Ttls | | | |
| | Tpsu | | | |
| | Tord | | | |
| | af | | | |
| | | | | |

**Table 2.2. Summary of Shear Strength Groups for the Niles Quadrangle.**

## PART II

## EARTHQUAKE-INDUCED LANDSLIDE HAZARD POTENTIAL

### Design Strong-Motion Record

The Newmark analysis used in delineating the earthquake-induced landslide zones requires the selection of a design earthquake strong-motion record. Because the active Hayward Fault traverses the western part of the Niles Quadrangle and the active Calaveras Fault traverses the northeastern part of the quadrangle, the selection of a strong motion record was based on the desire to simulate a large earthquake on one of these faults. The Hayward Fault is a right-lateral strike-slip fault with a total length of approximately 86 km and an estimated maximum moment magnitude of 7.1 (Petersen and others, 1996). The Calaveras Fault is also a right-lateral strike-slip fault with a total length of approximately 158 km and an estimated moment magnitude of 6.8 for the segment north of Calaveras Reservoir (Petersen and others, 1996). The hilly areas of the eastern Niles Quadrangle, which would be susceptible to earthquake-induced landsliding, range from zero to about 4 km from one or the other of these seismic sources. Strong-motion records considered in the selection include: the CGS Strong Motion Instrumentation Program (SMIP) Corralitos record from the 1989 Loma Prieta

earthquake; the Southern California Edison (SCE) Lucerne record from the 1992 Landers earthquake; and the Japan Meteorological Agency (JMA) Kobe City record from the 1995 Hyogoken-Nambu (Kobe) earthquake. The significant parameters for each of these earthquakes are listed below:

| Strong-Motion Record | Moment Magnitude | Source to Site Distance (km) | PGA (g) |
|---|---|---|---|
| SMIP Corralitos | 6.9 | 5.1 | 0.64 |
| SCE Lucerne | 7.3 | 1.1 | 0.80 |
| JMA Kobe | 6.9 | 0.6 | 0.82 |

The Corralitos record was eliminated because the fault motion was oblique, rather than purely strike-slip, and because of the relatively short rupture length. The Kobe record was eliminated because of uncertainties regarding the effects of topographic and basin-edge amplification at the recording site. Despite the slightly higher than expected magnitude, the Lucerne record from the 1992 Landers earthquake was used because it has many tectonic similarities to an earthquake on the Hayward Fault or the Calaveras Fault. The selected strong-motion record was not scaled or otherwise modified prior to analysis.

**Displacement Calculation**

The design strong-motion record was used to develop a relationship between landslide displacement and yield acceleration ($a_y$), defined as the earthquake horizontal ground acceleration above which landslide displacements take place. This relationship was prepared by integrating the design strong-motion record twice for a given acceleration value to find the corresponding displacement, and the process was repeated for a range of acceleration values (Jibson, 1993). The resulting curve in Figure 2.1 represents the full spectrum of displacements that can be expected for the design strong-motion record. This curve provides the required link between anticipated earthquake shaking and estimates of displacement for different combinations of geologic materials and slope gradient, as described in the Slope Stability Analysis section below.

The amount of displacement predicted by the Newmark analysis provides an indication of the relative amount of damage that could be caused by earthquake-induced landsliding. Displacements of 30, 15 and 5 cm were used as criteria for rating levels of earthquake-induced landslide hazard potential based on the work of Youd (1980), Wilson and Keefer (1983), and a CGS pilot study for earthquake-induced landslides (McCrink, 2001; McCrink and Real, 1996). Applied to the curve in Figure 2.1, these displacements correspond to yield accelerations of 0.14, 0.18 and 0.24g. Because these yield acceleration values are derived from the design strong-motion record, they represent the ground shaking opportunity thresholds that are significant in the Niles Quadrangle.

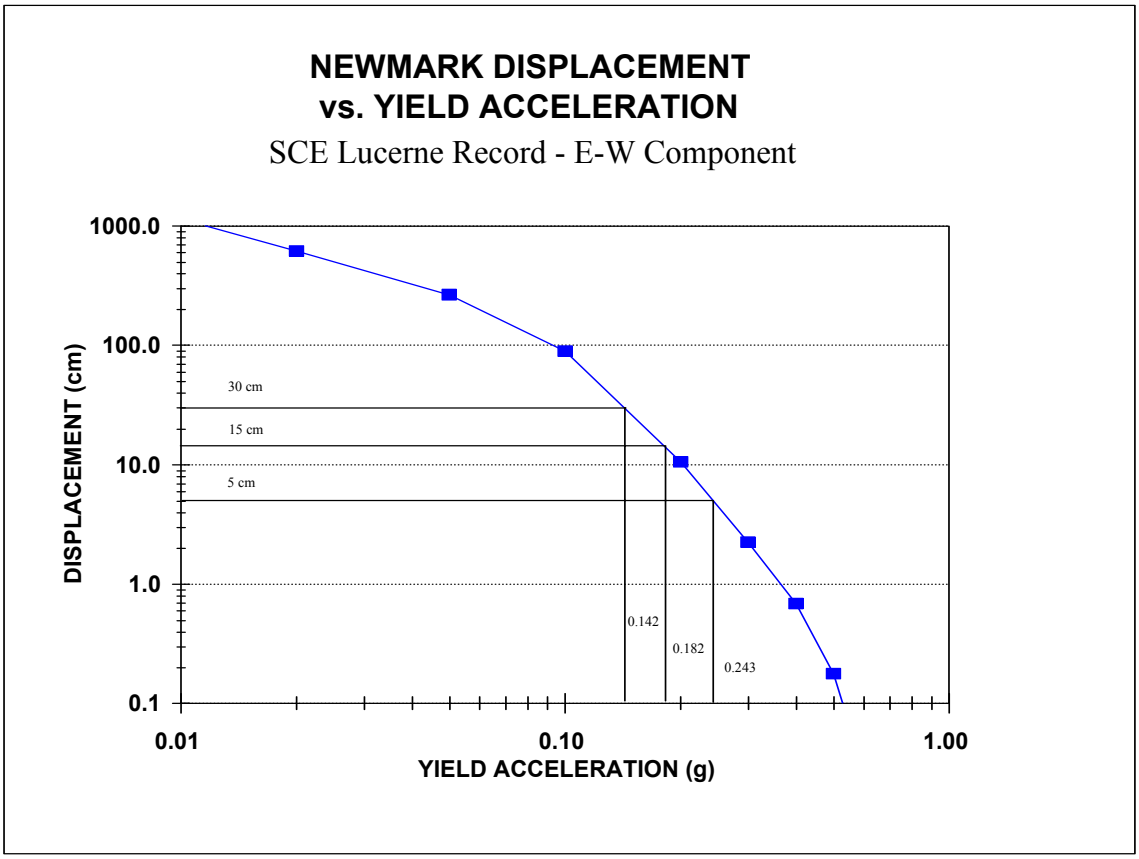


**Figure 2.1. Yield Acceleration vs. Newmark Displacement for the Lucerne Record for the 1992 Landers Earthquake.**

## Slope Stability Analysis

A slope stability analysis was performed for each geologic material strength group at slope increments of 1 degree. An infinite-slope failure model under unsaturated slope conditions was assumed. A factor of safety was calculated first, followed by the calculation of yield acceleration from Newmark's (1965) equation:

$$a_y = ( FS - 1 )g \sin \alpha$$

where **FS** is the Factor of Safety, **g** is the acceleration due to gravity, and $\alpha$ is the direction of movement of the slide mass, in degrees measured from the horizontal, when displacement is initiated (Newmark, 1965). For an infinite slope failure $\alpha$ is the same as the slope angle.

The yield accelerations resulting from Newmark's equations represent the susceptibility to earthquake-induced failure of each geologic material strength group for a range of

slope gradients. Based on the relationship between yield acceleration and Newmark displacement shown in Figure 2.1, hazard potentials were assigned as follows:

1. If the calculated yield acceleration was less than 0.14g, Newmark displacement greater than 30 cm is indicated, and a HIGH hazard potential was assigned (H on Table 2.3)

2. If the calculated yield acceleration fell between 0.14g and 0.18g, Newmark displacement between 15 cm and 30 cm is indicated, and a MODERATE hazard potential was assigned (M on Table 2.3)

3. If the calculated yield acceleration fell between 0.18g and 0.24g, Newmark displacement between 5 cm and 15 cm is indicated, and a LOW hazard potential was assigned (L on Table 2.3)

4. If the calculated yield acceleration was greater than 0.24g, Newmark displacement of less than 5 cm is indicated, and a VERY LOW potential was assigned (VL on Table 2.3)

Table 2.3 summarizes the results of the stability analyses. The earthquake-induced landslide hazard potential map was prepared by combining the geologic material-strength map and the slope map according to this table.

**NILES QUADRANGLE HAZARD POTENTIAL MATRIX**

| Geologic Material Strength Group (Average Phi) | HAZARD POTENTIAL (Percent Slope) | | | |
|---|---|---|---|---|
| | Very Low | Low | Moderate | High |
| 1 (32) | 0 to 38% | 38 to 45% | 45 to 49% | > 49% |
| 2 (28) | 0 to 29% | 29 to 34% | 34 to 38% | > 38% |
| 3 (23) | 0 to 19% | 19 to 25% | 25 to 29% | > 29% |
| 4 (18) | 0 to 6% | 6 to 13% | 13 to 19% | > 19% |
| 5 (12) | 0 | 0 | 0 to 6% | > 6% |

**Table 2.3. Hazard Potential Matrix for Earthquake-Induced Landslides in the Niles Quadrangle.** Values in the table show the range of slope gradient (expressed as percent slope) corresponding to calculated Newmark displacement ranges from the design earthquake for each material strength group.

# EARTHQUAKE-INDUCED LANDSLIDE HAZARD ZONE

## Criteria for Zoning

Earthquake-induced landslide zones were delineated using criteria adopted by the California State Mining and Geology Board (DOC, 2000). Under these criteria, earthquake-induced landslide hazard zones are defined as areas that meet one or both of the following conditions:

1. Areas that have been identified as having experienced landslide movement in the past, including all mappable landslide deposits and source areas as well as any landslide that is known to have been triggered by historic earthquake activity.

2. Areas where the geologic and geotechnical data and analyses indicate that the earth materials may be susceptible to earthquake-induced slope failure.

These conditions are discussed in further detail in the following sections.

## Existing Landslides

Existing landslides typically consist of disrupted soils and rock materials that are generally weaker than adjacent undisturbed rock and soil materials. Previous studies indicate that existing landslides can be reactivated by earthquake movements (Keefer, 1984). Earthquake-triggered movement of existing landslides is most pronounced in steep head scarp areas and at the toe of existing landslide deposits. Although reactivation of deep-seated landslide deposits is less common (Keefer, 1984), a significant number of deep-seated landslide movements have occurred during, or soon after, several recent earthquakes. Based on these observations, all existing landslides with a definite or probable confidence rating are included within the earthquake-induced landslide hazard zone.

## Geologic and Geotechnical Analysis

Based on the conclusions of a pilot study performed by CGS (McCrink, 2001; McCrink and Real, 1996), it has been concluded that earthquake-induced landslide hazard zones should encompass all areas that have a High, Moderate or Low level of hazard potential (see Table 2.3). This would include all areas where the analyses indicate earthquake displacements of 5 centimeters or greater. Areas with a Very Low hazard potential, indicating less than 5 centimeters displacement, are excluded from the zone.

As summarized in Table 2.3, all areas characterized by the following geologic strength group and slope gradient conditions are included in the earthquake-induced landslide hazard zone:

1. Geologic Strength Group 5 is included for all slope gradient categories. (Note: The only geologic unit included in Geologic Strength Group 5 is Qls, existing landslides.

They have been included or excluded from the landslide zones on the basis of the criteria described in the previous section)

2. Geologic Strength Group 4 is included for all slopes steeper than 6 percent.

3. Geologic Strength Group 3 is included for all slopes steeper than 19 percent.

4. Geologic Strength Group 2 is included for all slopes steeper than 29 percent.

5. Geologic Strength Group 1 is included for all slopes greater than 38 percent.

Based on these criteria, 36.5 percent of the Niles Quadrangle lies within earthquake-induced landslide hazard zones of required investigation.

## ACKNOWLEDGMENTS

The authors would like to thank the following individuals and organizations for their assistance in obtaining the data necessary to complete this project. Gary Moore and Mary Anne Hubbard with the County of Alameda arranged access and provided assistance in retrieving geotechnical data from files maintained by Alameda County. Andrew Russell with the city of Fremont arranged access and provided assistance in retrieving geotechnical data from files maintained by the city of Fremont. Ron Chan and Ron Fong with the city of Fremont generously provided digital terrain data for our analyses. At CGS, Terilee McGuire, Lee Wallinder and Bob Moscovitz provided GIS support. Harold Feinberg prepared the DEM from the city of Fremont terrain data. Barbara Wanish prepared the final landslide hazard zone maps and the graphic displays for this report. Al Barrows and Diane Vaughn edited and compiled this report for publication.

## REFERENCES

Andrews, J.D., Oppenheimer, D.H. and Lienkaemper, J.J., 1992, The Mission Link between the Hayward and Calaveras Faults: *in* Proceedings of the Second Conference on Earthquake Hazards in the Eastern San Francisco Bay Area, California Division of Mines and Geology Special Publication 113, p. 217-223.

Brabb, E.E., 1983, Map showing direction and amount of bedding dip of sedimentary rocks in San Mateo County, California: U.S. Geological Survey Miscellaneous Investigations Series Map I-1257C, 1 sheet, scale 1:62,500.

California Department of Conservation, Division of Mines and Geology, 1997a, Guidelines for evaluating and mitigating seismic hazards in California: California Division of Mines and Geology Special Publication 117, 74 p.

California Department of Conservation, Division of Mines and Geology, 1997b, Fault rupture hazard zones in California: California Division of Mines and Geology Special Publication 42, 38 p.

California Department of Conservation, Division of Mines and Geology, 2000, Recommended criteria for delineating seismic hazard zones: California Division of Mines and Geology Special Publication 118, 12 p.

Dibblee, T.W., Jr., 1980, Preliminary geologic map of the Niles Quadrangle, Alameda and Contra Costa counties, California: U.S. Geological Survey Open File Report 80-533C, scale 1:24,000.

Galehouse, J.S., 1992, Creep rates and creep characteristics of eastern San Francisco Bay area faults: 1979-1992 *in* Proceedings of the Second Conference on Earthquake Hazards in the Eastern San Francisco Bay Area, California Division of Mines and Geology Special Publication 113, p. 45-53.

Geolith Consultants, 2000, Mission Peak Landslide, Fremont, California: Unpublished consultant report prepared for the City of Fremont, February 2000.

Graymer, R., 1995, Geology of the Southeast San Francisco Bay Area Hills, California: *in* Sangines, E.M., Andersen, D.W. and Buising, A.B., *editors*, 1995, Recent geologic studies in the San Francisco Bay Area: Pacific Section Society of Economic Paleontologists and Mineralogists, v. 76, p. 115-124.

Graymer, R.W., 2000, Geologic map and map database of the Oakland metropolitan area, Alameda, Contra Costa, and San Francisco counties, California: U.S. Geological Survey Miscellaneous Field Studies MF-2342.

Graymer, R.W., Jones, D.L. and Brabb, E.E., 1996, Preliminary geologic map emphasizing bedrock formations in Alameda County, California: U.S. Geological Survey Digital Database Open File 96-252.

Horn, B.K.P., 1981, Hill shading and the reflectance map: Proceedings of the IEEE, v. 69, no. 1, p. 14-47.

Jibson, R.W., 1993, Predicting earthquake-induced landslide displacements using Newmark's sliding block analysis: Transportation Research Board, National Research Council, Transportation Research Record 1411, 17 p.

Jones, D.L. and Curtis, G.H., 1991, Guide to the geology of the Berkeley Hills, central Coast Ranges, California, *in* Sloan, Doris, and Wagner, D.L., *editors*, Geologic excursions in Northern California: San Francisco to the Sierra Nevada, California Division of Mines and Geology Special Publication 109, p. 63-74.

Keefer, D.K., 1984, Landslides caused by earthquakes: Geological Society of America Bulletin, v. 95, no. 4, p. 406-421.

Lienkaemper, J.J., 1992, Map showing recently active traces of the Hayward fault, Alameda and Contra Costa counties, California: U.S. Geological Survey Miscellaneous Field Studies Map MF-2196, 13 p., 1 sheet, scale 1:24,000.

Lienkaemper, J.J. and Borchardt, G., 1992, Hayward Fault: Large earthquakes versus surface creep: *in* Proceedings of the Second Conference on Earthquake Hazards in the Eastern San Francisco Bay Area, California Division of Mines and Geology Special Publication 113, p. 101-110.

McCrink, T.P., 2001, Mapping earthquake-induced landslide hazards in Santa Cruz County *in* Ferriz, H. and Anderson, R., *editors*, Engineering geology practice in northern California: California Geological Survey Bulletin 210 / Association of Engineering Geologists Special Publication 12, p.77-94.

McCrink, T.P. and Real, C.R., 1996, Evaluation of the Newmark method for mapping earthquake-induced landslide hazards in the Laurel 7-1/2 Minute Quadrangle, Santa Cruz County, California: California Division of Mines and Geology Final Technical Report for U.S. Geological Survey Contract 143-93-G-2334, U.S. Geological Survey, Reston, Virginia, 31 p.

Nilsen, T.H., 1975, Preliminary photointerpretation map of landslides and other surficial deposits of the Niles 7.5-Minute Quadrangle, Alameda County, California: U.S. Geological Survey Open-File Map 75-277, map # 40, scale 1:24,000.

Newmark, N.M., 1965, Effects of earthquakes on dams and embankments: Geotechnique, v. 15, no. 2, p. 139-160.

Petersen, M.D., Bryant, W.A., Cramer, C.H., Cao. T., Reichle, M.S., Frankel, A.D., Lienkaemper, J.J., McCrory, P.A. and Schwartz, D.P., 1996, Probabilistic seismic hazard assessment for the State of California: California Department of Conservation, Division of Mines and Geology, Open-File Report 96-08; also U.S. Geological Survey Open-File Report 96-706, 33 p.

Radbruch-Hall, D.H., 1974, Map showing recently active breaks along the Hayward fault zone and the southern part of the Calaveras fault zone, California: U.S. Geological Survey Miscellaneous Geologic Investigations Map I-813, scale 1:24,000.

Rogers, J.D. and Halliday, J.M., 1992, Tracking the elusive Calaveras Fault from Sunol to San Ramon: *in* Proceedings of the Second Conference on Earthquake Hazards in the Eastern San Francisco Bay Area, California Division of Mines and Geology Special Publication 113, p. 271-280.

Smith, T.C., 1980, Fault evaluation report FER-101: unpublished report, California Division of Mines and Geology, 30 p.

Smith, T.C., 1996, Preliminary maps of seismic hazard zones and draft guidelines for evaluating and mitigating seismic hazards: California Geology, v. 49, no. 6, p. 147-150.

Southern California Earthquake Center, 2002, Recommended procedures for implementation of DMG Special Publication 117 guidelines for analyzing and mitigating landslide hazards in California: Southern California Earthquake Center, University of Southern California, 108 p.

Sowers, J.M., unpublished mapping, to be incorporated in revision to Knudsen, K.L., Sowers, J.M., Witter, R.C., Wentworth, C.M., Helley, E.J., Nicholson, R.S., Wright, H.M. and Brown, K.H., 2000, Preliminary maps of Quaternary deposits and liquefaction susceptibility, nine-county San Francisco Bay region, California: a digital database, U.S. Geological Survey Open-File Report 00-444, scale 1:24,000

Trifunac, M.D., Todorovska, M.I. and Ivanovic, S.S., 1994, A note on distribution of uncorrected peak ground accelerations during the Northridge, California earthquake of 17 January 1994: Soil Dynamics and Earthquake Engineering, v. 13, no. 3, p. 187-196.

U.S. Geological Survey, 1993, Digital Elevation Models: National Mapping Program, Technical Instructions, Data Users Guide 5, 48 p.

Wilson, R.C. and Keefer, D.K., 1983, Dynamic analysis of a slope failure from the 1979 Coyote Lake, California, earthquake: Bulletin of the Seismological Society of America, v. 73, p. 863-877.

Wong, I.G. and Hemphill-Haley, M.A., 1992, Seismicity and faulting near the Hayward and Mission faults: *in* Proceedings of the Second Conference on Earthquake Hazards in the Eastern San Francisco Bay Area, California Division of Mines and Geology Special Publication 113, p. 207-215.

Youd, T.L., 1980, Ground failure displacement and earthquake damage to buildings: American Society of Civil Engineers Conference on Civil Engineering and Nuclear Power, 2d, Knoxville, Tennessee, 1980, v. 2, p. 7-6-2 to 7-6-26.

## AIR PHOTOS

United States Department of Agriculture (USDA), dated 7-26-39, Flight or Serial number BUT, Photo numbers 281-23-34, 281-45-55, 281-70-76, scale 1:20,000±.

United States Department of Agriculture (USDA), dated 6-8-40, Flight or Serial number BUT, Photo numbers 341-94-98, scale 1:20,000±.

WAC Corporation, Inc, dated 3-28-84, Flight or Serial number WAC 84C, Photo numbers 12-3-11, 11-214-223, scale 1:24,000±.

WAC Corporation, Inc, dated 4-23-02, Flight or Serial number WAC-C-02CA, Photo numbers 5-242-253, scale 1:24,000±.

WAC Corporation, Inc, dated 5-8-02, Flight or Serial number WAC-C-02CA, Photo numbers 9-20-31, 9-72-82, 9-122-133, scale 1:24,000±.

## APPENDIX A
## SOURCE OF ROCK STRENGTH DATA

| SOURCE | NUMBER OF TESTS SELECTED |
|---|---|
| County of Alameda | 160 |
| City of Hayward | 66 |
| City of Fremont | 57 |
| City of Union City | 12 |
| City of Milpitas | 8 |
| City of Oakland | 33 |
| Total Number of Shear Tests | 328 |

# SECTION 3
# GROUND SHAKING EVALUATION REPORT

## Potential Ground Shaking in the Niles 7.5-Minute Quadrangle, Alameda County, California

**By**

**Mark D. Petersen*, Chris H. Cramer*, Geoffrey A. Faneros, Charles R. Real, and Michael S. Reichle**

**California Department of Conservation**
**California Geological Survey**
***Formerly with CGS, now with U.S. Geological Survey**

### PURPOSE

The Seismic Hazards Mapping Act (the Act) of 1990 (Public Resources Code, Chapter 7.8, Division 2) directs the California Department of Conservation (DOC), Division of Mines and Geology (DMG) [now called California Geological Survey (CGS)] to delineate Seismic Hazard Zones. The purpose of the Act is to reduce the threat to public health and safety and to minimize the loss of life and property by identifying and mitigating seismic hazards. Cities, counties, and state agencies are directed to use the Seismic Hazard Zone Maps in their land-use planning and permitting processes. The Act requires that site-specific geotechnical investigations be performed prior to permitting most urban development projects within the hazard zones. Evaluation and mitigation of seismic hazards are to be conducted under guidelines established by the California State Mining and Geology Board (DOC, 1997). The text of this report is on the Internet at http://gmw.consrv.ca.gov/shmp/SHMPsp117.asp

This section of the evaluation report summarizes the ground motions used to evaluate liquefaction and earthquake-induced landslide potential for zoning purposes. Included are ground motion and related maps, a brief overview on how these maps were prepared, precautionary notes concerning their use, and related references. The maps provided

herein are presented at a scale of approximately 1:150,000 (scale bar provided on maps), and show the full 7.5-minute quadrangle and portions of the adjacent eight quadrangles. They can be used to assist in the specification of earthquake loading conditions ***for the analysis of ground failure*** according to the "Simple Prescribed Parameter Value" method (SPPV) described in the site investigation guidelines (DOC, 1997). Alternatively, they can be used as a basis for comparing levels of ground motion determined by other methods with the statewide standard.

This section and Sections 1 and 2 (addressing liquefaction and earthquake-induced landslide hazards) constitute a report series that summarizes development of seismic hazard zone maps in the state. Additional information on seismic hazard zone mapping in California can be accessed on the California Geological Survey's Internet page: http://www.consrv.ca.gov/CGS/index.htm

## EARTHQUAKE HAZARD MODEL

The estimated ground shaking is derived from the statewide probabilistic seismic hazard evaluation released cooperatively by the California Department of Conservation, Division of Mines and Geology [California Geological Survey], and the U.S. Geological Survey (Petersen and others, 1996). That report documents an extensive 3-year effort to obtain consensus within the scientific community regarding fault parameters that characterize the seismic hazard in California. Fault sources included in the model were evaluated for long-term slip rate, maximum earthquake magnitude, and rupture geometry. These fault parameters, along with historical seismicity, were used to estimate return times of moderate to large earthquakes that contribute to the hazard.

The ground shaking levels are estimated for each of the sources included in the seismic source model using attenuation relations that relate earthquake shaking with magnitude, distance from the earthquake, and type of fault rupture (strike-slip, reverse, normal, or subduction). The published hazard evaluation of Petersen and others (1996) only considers uniform firm-rock site conditions. In this report, however, we extend the hazard analysis to include the hazard of exceeding peak horizontal ground acceleration (PGA) at 10 percent probability of exceedance in 50 years on spatially uniform conditions of rock, soft rock, and alluvium. These soil and rock conditions approximately correspond to site categories defined in Chapter 16 of the Uniform Building Code (ICBO, 1997), which are commonly found in California. We use the attenuation relations of Boore and others (1997), Campbell (1997), Sadigh and others (1997), and Youngs and others (1997) to calculate the ground motions.

The seismic hazard maps for ground shaking are produced by calculating the hazard at sites separated by about 5 km. Figures 3.1 through 3.3 show the hazard for PGA at 10 percent probability of exceedance in 50 years assuming the entire map area is firm rock, soft rock, or alluvial site conditions respectively. The sites where the hazard is calculated are represented as dots and ground motion contours as shaded regions. The quadrangle of interest is outlined by bold lines and centered on the map. Portions of the eight

NILES 7.5 MINUTE QUADRANGLE AND PORTIONS OF
ADJACENT QUADRANGLES

*10% EXCEEDANCE IN 50 YEARS PEAK GROUND ACCELERATION (g)*

1998

**FIRM ROCK CONDITIONS**

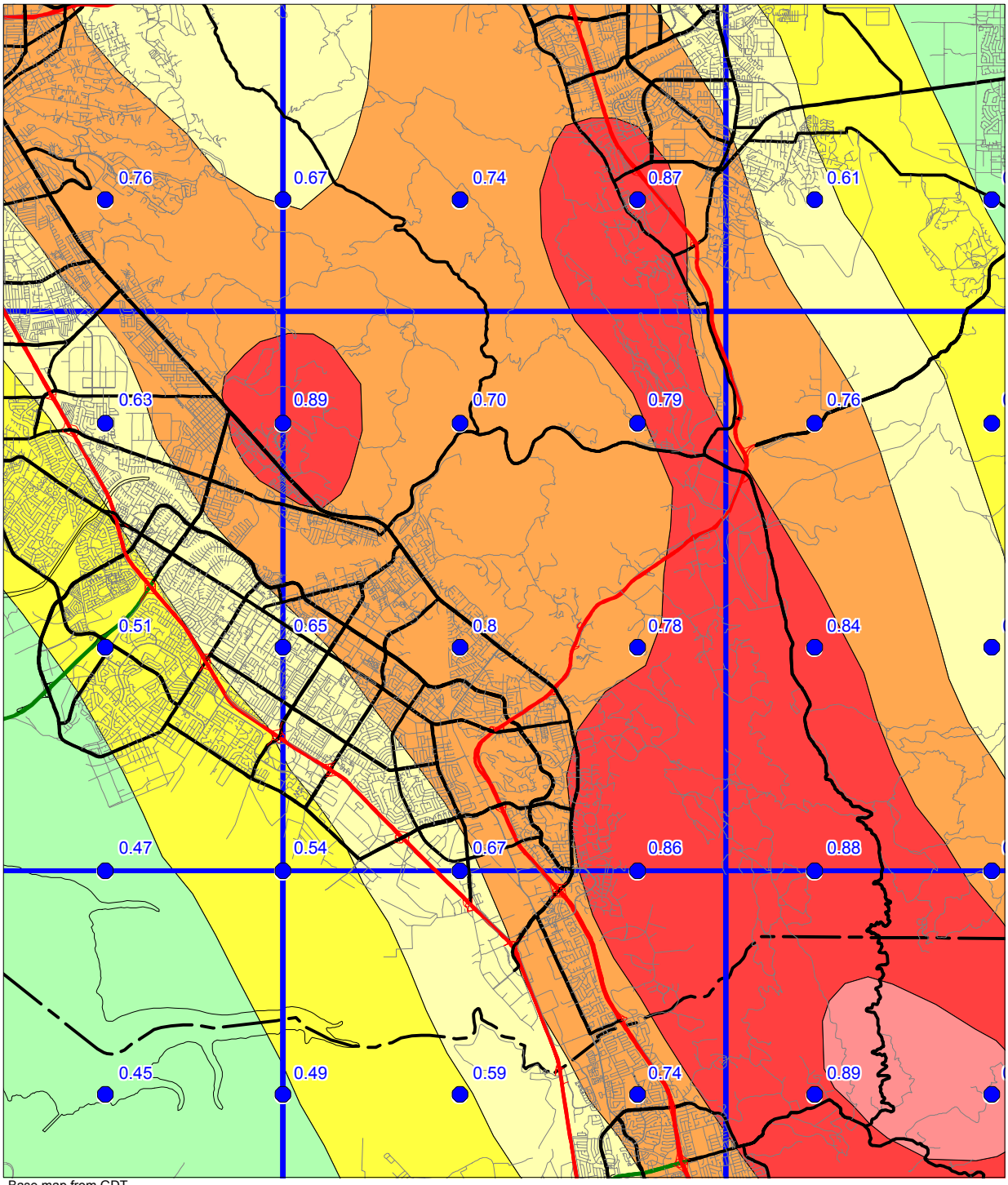


Base map from GDT

0 1.5 3
Miles

Department of Conservation
California Geological Survey

Figure 3.1

NILES 7.5 MINUTE QUADRANGLE AND PORTIONS OF
ADJACENT QUADRANGLES

*10% EXCEEDANCE IN 50 YEARS PEAK GROUND ACCELERATION (g)*

1998

**SOFT ROCK CONDITIONS**

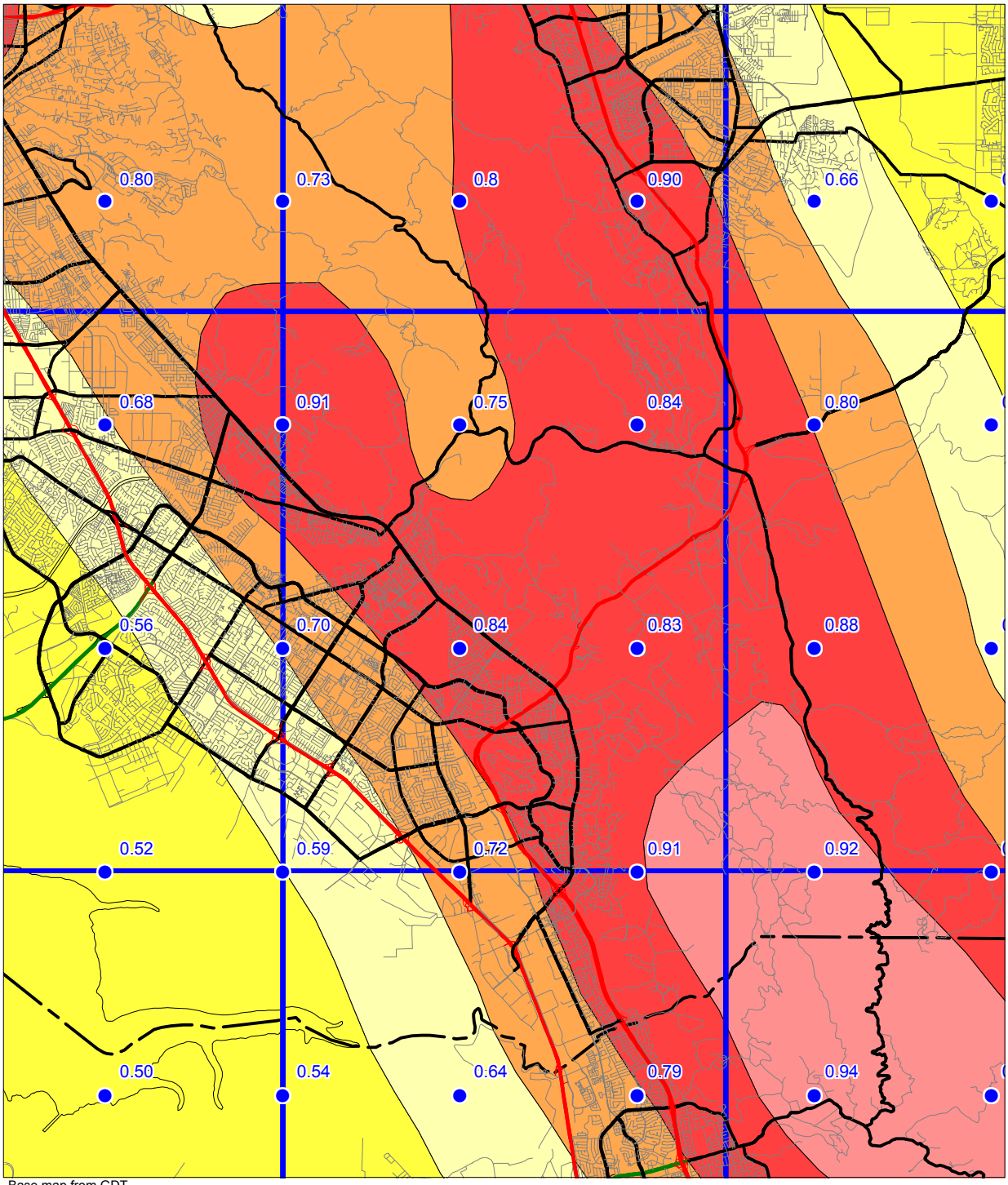


Base map from GDT

0 1.5 3
Miles

Department of Conservation
California Geological Survey

Figure 3.2

NILES 7.5 MINUTE QUADRANGLE AND PORTIONS OF
ADJACENT QUADRANGLES

*10% EXCEEDANCE IN 50 YEARS PEAK GROUND ACCELERATION (g)*
1998

**ALLUVIUM CONDITIONS**

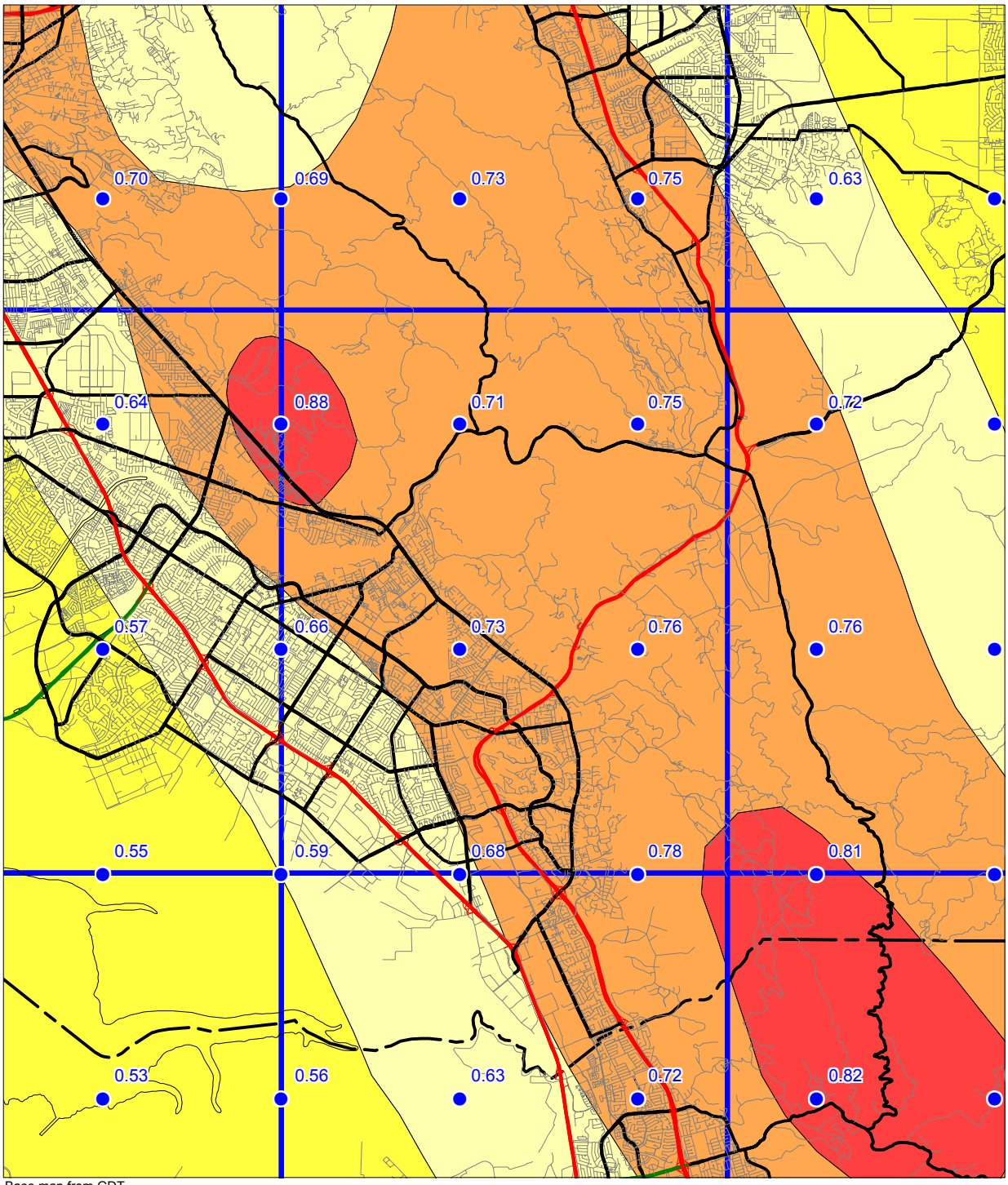


Base map from GDT

0 1.5 3
Miles

Department of Conservation
California Geological Survey

Figure 3.3

adjacent quadrangles are also shown so that the trends in the ground motion may be more apparent. We recommend estimating ground motion values by selecting the map that matches the actual site conditions, and interpolating from the calculated values of PGA rather than the contours, since the points are more accurate.

## APPLICATIONS FOR LIQUEFACTION AND LANDSLIDE HAZARD ASSESSMENTS

Deaggregation of the seismic hazard identifies the contribution of each of the earthquakes (various magnitudes and distances) in the model to the ground motion hazard for a particular exposure period (see Cramer and Petersen, 1996). The map in Figure 3.4 identifies the magnitude and the distance (value in parentheses) of the earthquake that contributes most to the hazard at 10 percent probability of exceedance in 50 years on alluvial site conditions (*predominant earthquake*). This information gives a rationale for selecting a seismic record or ground motion level in evaluating ground failure. However, it is important to keep in mind that more than one earthquake may contribute significantly to the hazard at a site, and those events can have markedly different magnitudes and distances. For liquefaction hazard the predominant earthquake magnitude from Figure 3.4 and PGA from Figure 3.3 (alluvium conditions) can be used with the Youd and Idriss (1997) approach to estimate cyclic stress ratio demand. For landslide hazard the predominant earthquake magnitude and distance can be used to select a seismic record that is consistent with the hazard for calculating the Newmark displacement (Wilson and Keefer, 1983). When selecting the predominant earthquake magnitude and distance, it is advisable to consider the range of values in the vicinity of the site and perform the ground failure analysis accordingly. This would yield a range in ground failure hazard from which recommendations appropriate to the specific project can be made. Grid values for predominant earthquake magnitude and distance should **not** be interpolated at the site location, because these parameters are not continuous functions.

A preferred method of using the probabilistic seismic hazard model and the "simplified Seed-Idriss method" of assessing liquefaction hazard is to apply magnitude scaling probabilistically while calculating peak ground acceleration for alluvium. The result is a "magnitude-weighted" ground motion (liquefaction opportunity) map that can be used directly in the calculation of the cyclic stress ratio threshold for liquefaction and for estimating the factor of safety against liquefaction (Youd and Idriss, 1997). This can provide a better estimate of liquefaction hazard than use of predominate magnitude described above, because all magnitudes contributing to the estimate are used to weight the probabilistic calculation of peak ground acceleration (Real and others, 2000). Thus, large distant earthquakes that occur less frequently but contribute *more* to the liquefaction hazard are appropriately accounted for.

Figure 3.5 shows the magnitude-weighted alluvial PGA based on Idriss' weighting function (Youd and Idriss, 1997). It is important to note that the values obtained from this map are pseudo-accelerations and should be used in the formula for factor of safety without any magnitude-scaling (a factor of 1) applied.

NILES 7.5 MINUTE QUADRANGLE AND PORTIONS OF
ADJACENT QUADRANGLES

*10% EXCEEDANCE IN 50 YEARS PEAK GROUND ACCELERATION*

1998

**PREDOMINANT EARTHQUAKE**
**Magnitude (Mw)**
**(Distance (km))**

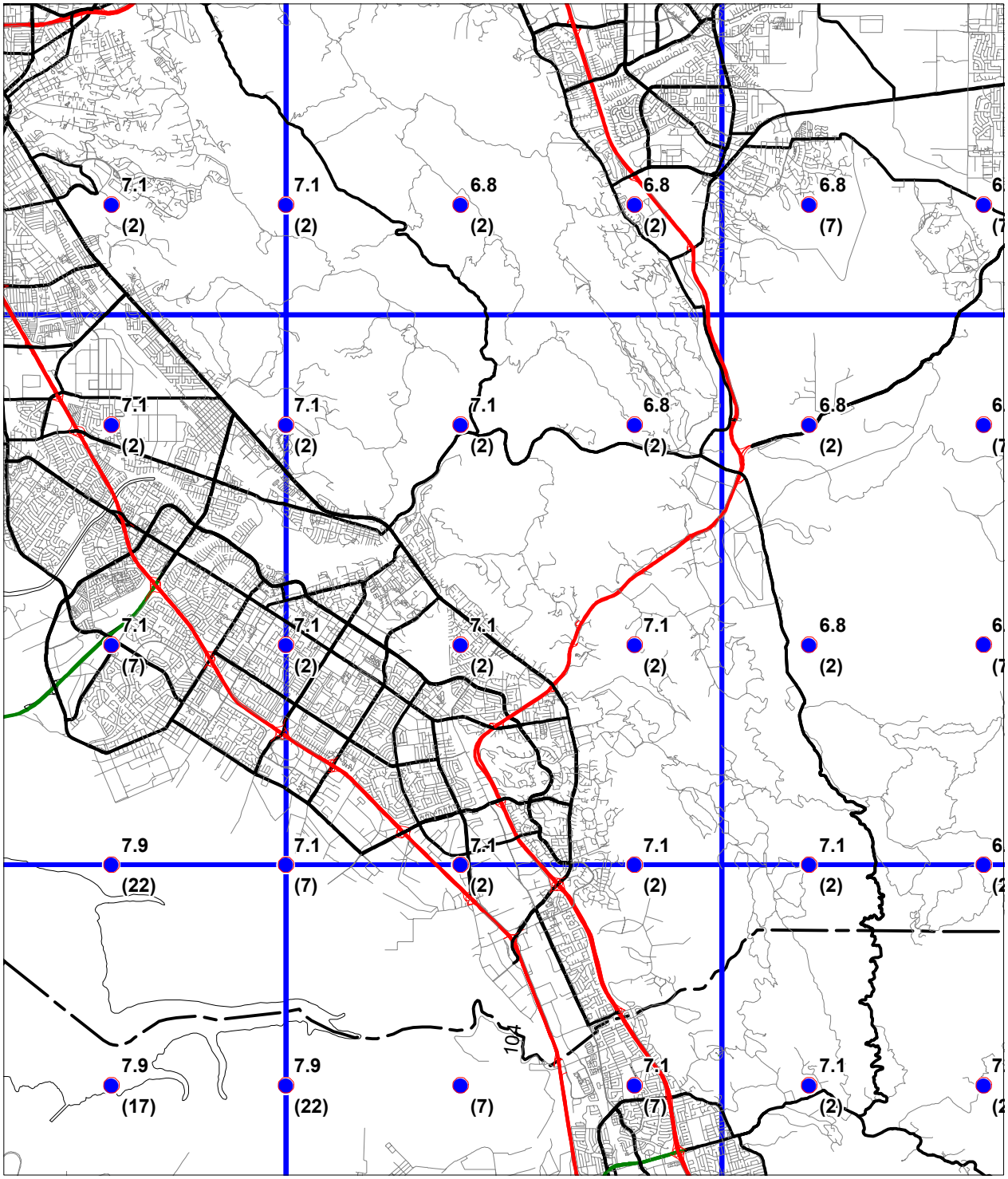


Base map from GDT

0 1.5 3
Miles

Department of Conservation
California Geological Survey
Figure 3.4

NILES 7.5 MINUTE QUADRANGLE AND PORTIONS OF
ADJACENT QUADRANGLES

*10% EXCEEDANCE IN 50 YEARS MAGNITUDE-WEIGHTED PSEUDO-PEAK ACCELERATION (g)*
*FOR ALLUVIUM*

1998

**LIQUEFACTION OPPORTUNITY**

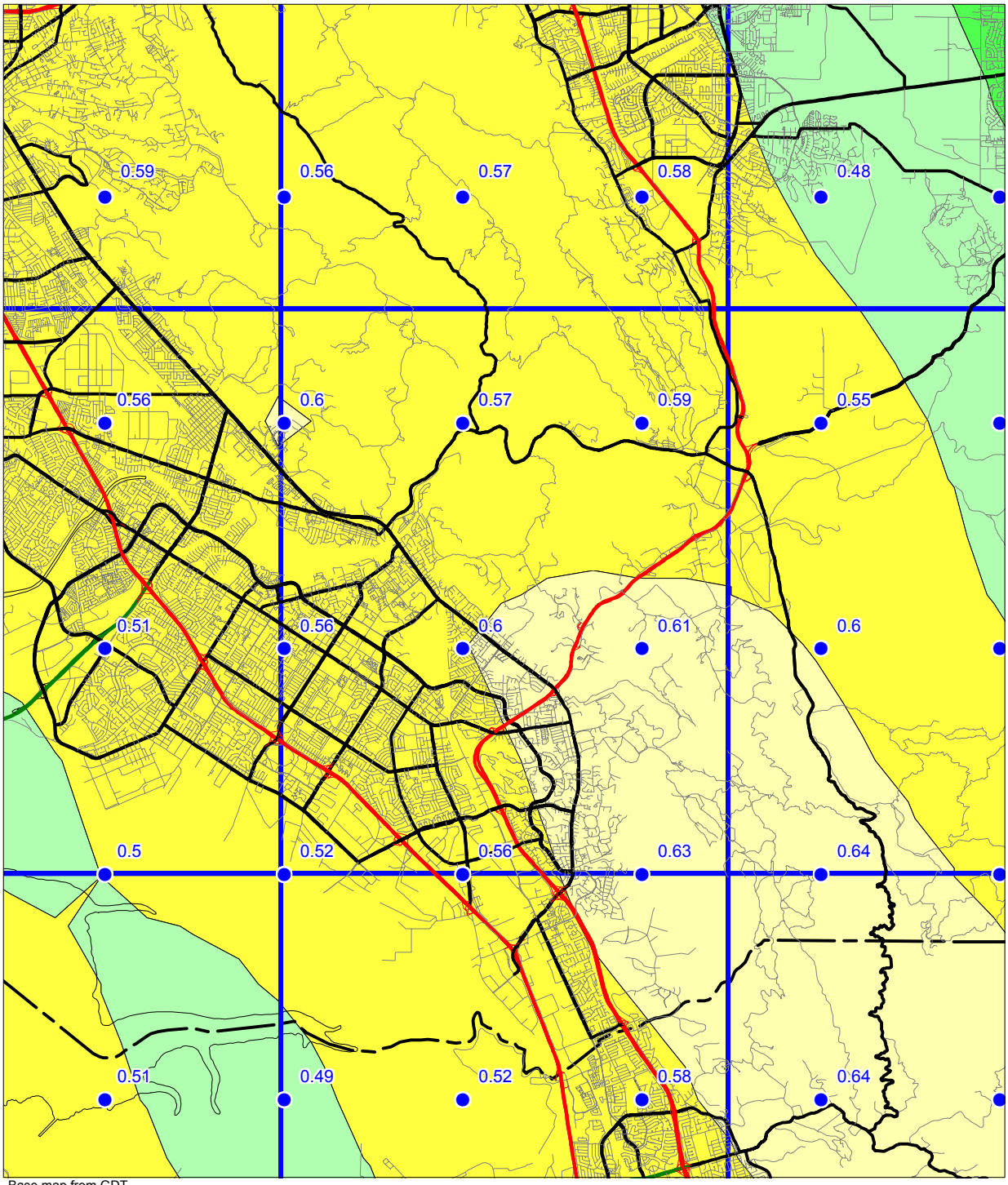


Base map from GDT

0 1.5 3
Miles

Department of Conservation
California Geological Survey

Figure 3.5

## USE AND LIMITATIONS

The statewide map of seismic hazard has been developed using regional information and is ***not appropriate for site specific structural design applications***. Use of the ground motion maps prepared at larger scale is limited to estimating earthquake loading conditions for preliminary assessment of ground failure at a specific location. We recommend consideration of site-specific analyses before deciding on the sole use of these maps for several reasons.

1. The seismogenic sources used to generate the peak ground accelerations were digitized from the 1:750,000-scale fault activity map of Jennings (1994). Uncertainties in fault location are estimated to be about 1 to 2 kilometers (Petersen and others, 1996). Therefore, differences in the location of calculated hazard values may also differ by a similar amount. At a specific location, however, the log-linear attenuation of ground motion with distance renders hazard estimates less sensitive to uncertainties in source location.

2. The hazard was calculated on a grid at sites separated by about 5 km (0.05 degrees). Therefore, the calculated hazard may be located a couple kilometers away from the site. We have provided shaded contours on the maps to indicate regional trends of the hazard model. However, the contours only show regional trends that may not be apparent from points on a single map. Differences of up to 2 km have been observed between contours and individual ground acceleration values. *We recommend that the user interpolate PGA between the grid point values rather than simply using the shaded contours*.

3. Uncertainties in the hazard values have been estimated to be about +/- 50 percent of the ground motion value at two standard deviations (Cramer and others, 1996).

4. Not all active faults in California are included in this model. For example, faults that do not have documented slip rates are not included in the source model. Scientific research may identify active faults that have not been previously recognized. Therefore, future versions of the hazard model may include other faults and omit faults that are currently considered.

5. A map of the predominant earthquake magnitude and distance is provided from the deaggregation of the probabilistic seismic hazard model. However, it is important to recognize that a site may have more than one earthquake that contributes significantly to the hazard. Therefore, in some cases earthquakes other than the predominant earthquake should also be considered.

Because of its simplicity, it is likely that the SPPV method (DOC, 1997) will be widely used to estimate earthquake shaking loading conditions for the evaluation of ground failure hazards. It should be kept in mind that ground motions at a given distance from an earthquake will vary depending on site-specific characteristics such as geology, soil properties, and topography, which may not have been adequately accounted for in the regional hazard analysis. Although this variance is represented to some degree by the

recorded ground motions that form the basis of the hazard model used to produce Figures 3.1, 3.2, and 3.3, extreme deviations can occur. More sophisticated methods that take into account other factors that may be present at the site (site amplification, basin effects, near source effects, etc.) should be employed as warranted. The decision to use the SPPV method with ground motions derived from Figures 3.1, 3.2, or 3.3 should be based on careful consideration of the above limitations, the geotechnical and seismological aspects of the project setting, and the "importance" or sensitivity of the proposed building with regard to occupant safety.

## REFERENCES

Boore, D.M., Joyner, W.B. and Fumal, T.E., 1997, Empirical near-source attenuation relationships for horizontal and vertical components of peak ground acceleration, peak ground velocity, and pseudo-absolute acceleration response spectra: Seismological Research Letters, v. 68, p. 154-179.

California Department of Conservation, Division of Mines and Geology, 1997, Guidelines for evaluating and mitigating seismic hazards in California: Special Publication 117, 74 p.

Campbell, K.W., 1997, Attenuation relationships for shallow crustal earthquakes based on California strong motion data: Seismological Research Letters, v. 68, p. 180-189.

Cramer, C.H. and Petersen, M.D., 1996, Predominant seismic source distance and magnitude maps for Los Angeles, Orange and Ventura counties, California: Bulletin of the Seismological Society of America, v. 85, no. 5, p. 1645-1649.

Cramer, C.H., Petersen, M.D. and Reichle, M.S., 1996, A Monte Carlo approach in estimating uncertainty for a seismic hazard assessment of Los Angeles, Ventura, and Orange counties, California: Bulletin of the Seismological Society of America, v. 86, p. 1681-1691.

International Conference of Building Officials (ICBO), 1997, Uniform Building Code: v. 2, Structural engineering and installation standards, 492 p.

Jennings, C.W., *compiler*, 1994, Fault activity map of California and adjacent areas: California Department of Conservation, Division of Mines and Geology, California Geologic Data Map Series, map no. 8.

Petersen, M.D., Bryant, W.A., Cramer, C.H., Cao, T., Reichle, M.S., Frankel, A.D., Lienkaemper, J.J., McCrory, P.A. and Schwartz, D.P., 1996, Probabilistic seismic hazard assessment for the State of California: California Department of Conservation, Division of Mines and Geology Open-File Report 96-08; also U.S. Geological Survey Open-File Report 96-706, 33 p.

Real, C.R., Petersen, M.D., McCrink, T.P. and Cramer, C.H., 2000, Seismic Hazard Deaggregation in zoning earthquake-induced ground failures in southern California: Proceedings of the Sixth International Conference on Seismic Zonation, November 12-15, Palm Springs, California, EERI, Oakland, CA.

Sadigh, K., Chang, C.-Y., Egan, J.A., Makdisi, F. and Youngs, R.R., 1997, SEA96- A new predictive relation for earthquake ground motions in extensional tectonic regimes: Seismological Research Letters, v. 68, p. 190-198.

Wilson, R.C. and Keefer, D.K., 1983, Dynamic analysis of a slope failure from the 1979 Coyote Lake, California, Earthquake: Bulletin of the Seismological Society of America, v. 73, p. 863-877.

Youd, T.L. and Idriss I.M., 1997, Proceedings of the NCEER workshop on evaluation of liquefaction resistance of soils: Technical Report NCEER-97-0022, 40 p.

Youngs, R.R., Chiou, S.-J., Silva, W.J. and Humphrey, J.R., 1997, Stochastic point-source modeling of ground motions in the Cascadia Region: Seismological Research Letters, v. 68, p. 74-85.

Base map enlarged from U.S.G.S. 30 x 60-minute series

## NILES QUADRANGLE

SCALE

1 .5 0 1 MILE

1000 0 1000 2000 3000 4000 5000 6000 7000 FEET

1 .5 0 1 KILOMETER

N

Hayward and Calaveras Faults from Bryant and others (2001)

B = Pre-Quaternary bedrock.

See "Bedrock and Surficial Geology" in Section 1 of report for descriptions of units.

Plate 1.1 Quaternary Geologic Map of the Niles 7.5-Minute Quadrangle, modified from J. Sowers (unpublished mapping).

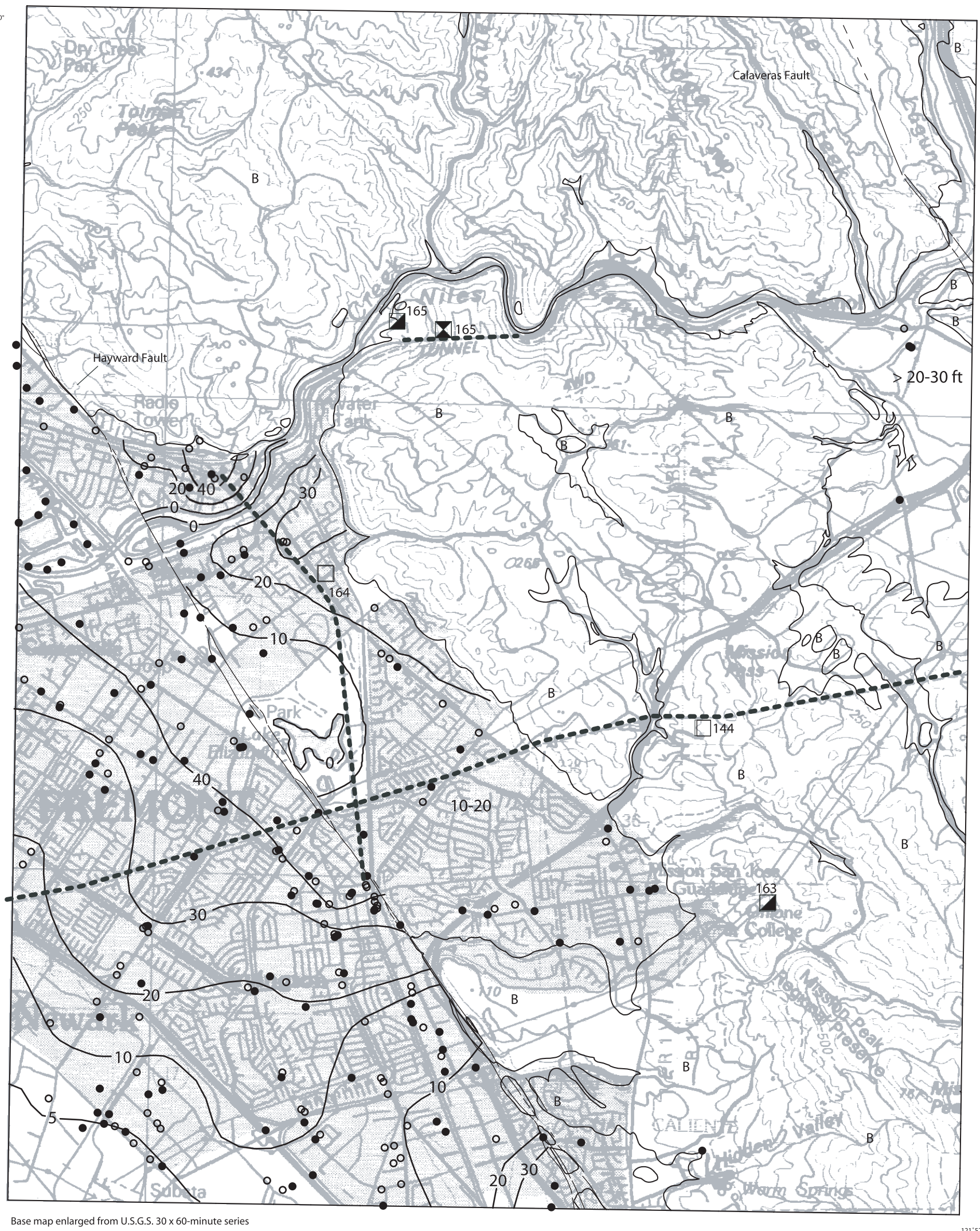


Base map enlarged from U.S.G.S. 30 x 60-minute series

NILES QUADRANGLE

SCALE

N

Ground Failures

- Miscellaneous effects
- Hillside Landslides
- Absence of ground failure
- Extent of ground failure

B = Pre-Quaternary bedrock.
See "Bedrock and Surficial Geology" in Section 1 of report for descriptions of units.

- Geotechnical borings used in liquefaction evaluation
- Regional Water Quality Control Board ground-water level measurements
- 50 — Depth to ground water, in feet

Plate 1.2 Depth to historically high ground water, and locations of boreholes used in this study, Niles 7.5-Minute Quadrangle, California. Hayward and Calaveras Faults from Bryant and others (2001).

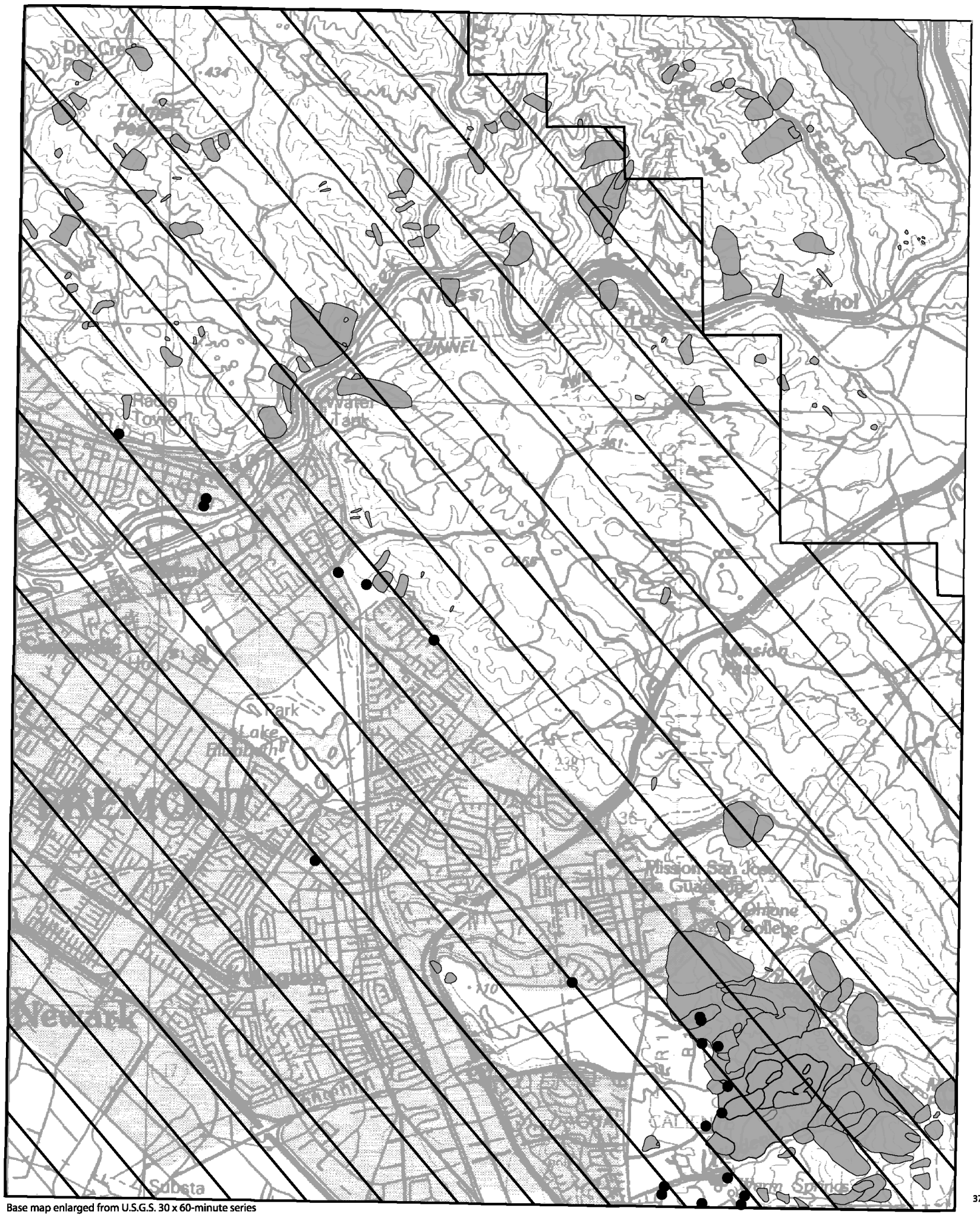


Plate 2.1 Landslide inventory, shear test sample locations, and areas of significant grading, Niles 7.5-Minute Quadrangle, California.